INDIAN JOURNAL OF SCIENCE AND TECHNOLOGY

RESEARCH ARTICLE

Comparative Study of Solar PV System Performance under Partial Shaded Condition Utilizing Different Control Approaches

AL-Wesabi Ibrahim[1,2]*, Zhijian Fang[1,2], Khaled Ameur[3], Ding Min[1,2], M B Shafik[4], Galal Al-Muthanna[5]

1 School of Automation, China University of Geoscience, Wuhan, 430074, China
2 Hubei Key Laboratory of Advanced Control and Intelligent Automation for Complex Systems, Wuhan, 430074, China
3 LACoSERE Laboratory, Amar Telidji University, Laghouat, Algeria
4 Electric power system and machines department, Faculty of Engineering, Kafrelsheikh University, Kafrelsheikh, 33516, Egypt
5 School of electrical engineering, southeast university, Nanjing, 210096, China

OPEN ACCESS

Received: 22.05.2021
Accepted: 05.06.2021
Published: 01.07.2021

Citation: Ibrahim ALW, Fang Z, Ameur K, Min D, Shafik MB, Al-Muthanna G (2021) Comparative Study of Solar PV System Performance under Partial Shaded Condition Utilizing Different Control Approaches. Indian Journal of Science and Technology 14(22): 1864-1893. https://doi.org/10.17485/IJST/v14i22.827

* **Corresponding author**.

fzjwhu@foxmail.com

Funding: Hubei Provincial Natural Science Foundation of China (2015CFA010), the Technology Project of State Grid Company "Soft Connection Mechanism and Modeling of Smart Grid Adapting to the Development of Global Energy Interconnection," and the 111 Projects (B17040)

Competing Interests: None

Published By Indian Society for Education and Environment (iSee)

ISSN
Print: 0974-6846
Electronic: 0974-5645

Abstract

Objectives: To improve the reduction of photovoltaic system's power output under various resistance load. Additionally, partial shaded conditions (PSCs) lead to several peaks on photovoltaic (PV) curves, which decrease conventional techniques' efficiency and in these (PSCs), standard equations might not be implemented entirely, therefore, the mathematical model of PV array is compulsory to modify and re-establish as well as it is compulsory to apply some methods based on artificial intelligence to develop the performance of traditional techniques. **Methods**: This work has modified and re-established the mathematical model of PV array under (PSCs) which are recognized and verified using MATLAB/Simulink environment. Also, heuristic algorithms (Cuckoo Search Algorithm (CSA) and Modified Particle Swarm Optimization (MPSO)) have been suggested and applied with PV system to promote output power under various resistance load, varying weather conditions and (PSCs). Moreover, these suggested algorithms can improve the dynamic response and steady-state PV systems' performance simultaneously and effectively comparing to the Modified Perturb and Observe (MP&O) and Artificial Neural Network (ANN) methods. **Findings**: The proposed methods are examined under various resistance load, several scenarios for (PSCs) and non-uniform irradiation levels to investigate its effectiveness. The results ensure that proposed tracker based on Cuckoo Search Algorithm (CSA) can distinguish between the global and local maximum peaks of PV system effectively with efficiency of 99% comparing to other MPPT approaches. So, all approaches mentioned above are implemented to improve the output power of PV system in Yemen. **Novelty:** Modified and re-established the mathematical model of PV array under (PSCs) and also, proposed a heuristic algorithms (CSA) and (MPSO))

to apply with PV system to promote maximum output power under various resistance load, varying weather conditions and (PSCs) as well as to improve the performance of (MP&O) and (ANN) methods.

Keywords: PV Systems; Maximum Power Point Tracking (MPPT); Uniform Irradiation; Partial Shading; Cuckoo Search Algorithm (CSA); MPSO; ANN; and MP&O

1 Introduction

The applications for PV solar systems are increasing, which need to develop the ingredients and methods used to harness this power source. PV system efficiency, the intensity of source irradiation, and storage methods are the main aspects that disturb the effectiveness of the collection process. The efficiency of a PV is limited by materials used in photovoltaic manufacturing. It is practically hard to do significant enhancements in the cell's performance, hence controlling the global gathering procedure's effectiveness. Therefore, the most available method to improve the solar power system's performance is the rise of irradiation intensity [1].

The total amount of sunlight is mostly existing, and it does have the potential to meet a considerable amount of power demand around the world. Over time the use of Solar panels is spreading particularly throughout too many of the rural areas but what remains as a back flaw is these panels' ability to harness that sunlight with proper efficiency and use it properly. Solar energy (SE) is the optimum solution that can provide griddles power and completely clean pollution and health hazards. Even after having too many solar energy features, it is still not as widely used as possible. The central aspect of concern remains in terms of its efficiency and another big question about its operation during uniform and non-uniform radiation conditions and conditions of partial shading [2,3].

Due to Yemen's current situation, the power grid has stopped working, and no energy projects have been added to the system. Besides, the increasing demand for electrical power increase because of an increase in population. Moreover, fossil fuels always hard to find, and fuel shortages frequently happened. Therefore, Yemeni people depend on renewable resources as primary energy resources. However, there are no rivers in Yemen, and wind speed cannot produce efficient power in most areas. So, solar energy has been considered the dominant and optimal power source. Solar energy is not only used for homes but also primarily used for farm water pumps. Yemen has excellent solar resources potential, and the solar system is an area where there is much progress. The apparent disadvantage of solar systems is the general low efficiency. These facts make the study of introducing more efficient solar systems in Yemen, and providing background for power engineers is significant.

Yemen belongs to the global sun-belt with average sunshine 9-11 hour/day and the peak sun hour (PSH) reach 6-7 hours with annual direct average energy density 1600-2200 kWh/m^2, which makes the less cost of power than any other country with less PSH. This geographical position encourages Yemeni people to use solar energy applications. The generation of electricity from solar energy using PV has low efficiency. Nevertheless, to improve the PV utilization, the system should operate around the MPP by proper MPPT technique.

All of the matters mentioned above, the design of an MPPT solar charge controller is essential to increase the PV solar system's efficiency output. Besides, force the PV array to operate as much as possible at the peak level of power. These MPPT techniques have also been proposed to regulate charging rates depending on the battery's charge level to allow charging closer to the battery's maximum capacity and supervise battery temperature to prohibit overheating. Moreover, the MPPT methods are the best decision for colder conditions; PV array voltage can be more significant than battery voltage;

hence the MPPT solar charge controller will harvest more power from the solar array. An MPPT solar charging controller for photovoltaic is an excellent feature of this controller in the panel, which may only improve the maximum potential of using solar panels [4,5]. It inspired me to execute the Cuckoo Search Algorithm and compared it with Modified Particle Swarm Optimization, ANN, and MP&O techniques to governor the GMPP of photovoltaic systems.

Cuckoo Search is an optimization method that is motivated by the natural parasitic reproduction strategy of cuckoo birds. This method is similar to the genetic algorithm (GA) and particle swarm optimization depending on the population algorithm; it also has some similarity to the harmony search in the selection procedure. The randomization is made much more efficient by Levy flight, which gives faster convergence. Also, the number of tuning parameters (two parameters) in this method is less than that in GA and PSO (three parameters and more). In addition, the characteristic of the Cuckoo search does not depend on giving the samples initial values [6]. When using the Cuckoo search method to get the global peak of the maximum power of PV arrays under partial shading conditions, the search process has to be made by choosing suitable variables. The output voltage and step size are the two parameters of the Cuckoo search algorithm. If the new sample is more than the old sample, then the new sample's maximum power is selected as the new best sample. If the new sample has a lesser amount than the old sample, the maximum power is kept. The course continues until all samples have reached the MPP [6–10].

Recently, several studies on another soft computing method called the cuckoo Search Algorithm (CSA) have attracted significant attention [11]. CSA has been more robust, convergent, and efficient [12]. Also, it requires fewer tuning parameters, which is an advantage of considering the rapid design process. After a thorough search, it was determined that the use of CSA for MPPT was reported in some technical publications elsewhere, and it gives a beautiful result in the field of MPPT. So, we used MPPT-CSA to improve Yemen's PV utilization system to make the PV system operate around the MPP. Therefore, based on the literature gap, this work can be implemented. This paper's main contribution is to establish the feasibility of multi-point tracking and realize it in the existing photovoltaic system.

Furthermore, to prove its feasibility, we evaluated three mature MPPT methods, MPSO, MP&O, and ANN. Several performance tests were executed, i.e., its operation during uniform and non-uniform radiation conditions, partial shading conditions, and changing loads. Finally, the prospect of CSA as the MPPT algorithm in a photovoltaic system is discussed and suggested.

2 Related work

The P–V characteristics curve shows a nonlinear, time-varying maximum power point (MPP) issue because of the persistent variation in the weather condition. Firstly, the temperature and solar irradiance and secondly PSCs, which is the most important reason behind MPP's problems in the PV curve features. Therefore, many different MPPT techniques have been proposed to guarantee that the PV arrays are feeding the load demand with the always required maximum power point (MPP) and used in integration with the power converter (DC-DC converter and inverter). These MPPT techniques are reported in the literature and classified into either conventional MPPT or soft computing methods. The existing techniques vary in simplicity, accuracy, time response, popularity, cost, and other technical aspects [13].

In [14,15], conventional MPPT methods and soft computing methods have been studied and reviewed outstandingly. For conventional MPPT, the three most popular techniques widely used are Perturb and Observe (P&O) [16], Hill Climbing (HC) [17], and Incremental Conductance (In-Cond) [18]. Besides, there are other more straightforward techniques such as the fractional short circuit current [19], fractional open circuit voltage [20], ripple correlation control [21], sliding control [22], and mathematical-graphical approach [23]. However, when the enticement condition changes (non-uniform irradiance) and PSCs occurred in part or the whole module of the PV array, the MPPT around (MPP) point's efficiency is challenged. At the same time, the oscillation of waveform near MPP is the main disadvantage of these algorithms. This oscillation near the MPPT results in an increase in power loss during steady-state, which dramatically reduces the system's efficiency. Besides, these methods can be confused when environmental conditions change because the operating point may leave the MPP rather than continue to work around it. Under normal conditions, i.e., uniform irradiance, they can track MPP effectively and have good convergence speed [24]. Finally, conventional MPPT methods cannot deal with partial shading conditions and non-uniform irradiance [25]. Many works have necessarily been executed to diminish the fluctuation and oscillation of these methods. In [26], A solar tracker and an improved Perturbation observation (P & O) algorithm for stand-alone photovoltaic power generation systems are proposed. The algorithm limits the power curve's search space to 10% of the maximum power point (MPP) and begins to disturb and observe in the limited search space. Therefore, the integration of solar tracker and improved P & O MPPT algorithm can better load quality, regulate power, and reduce steady-state oscillation at MPP. In [27–31], the traditional MPPT methods are modified to improve the efficiency and performance of these methods, which is an improved P & O (MPPT) method based on the adaptive duty cycle step of fuzzy logic controller [27]. A direct control IC MPPT algorithm based on Fuzzy duty cycle change estimator is proposed [28]. Some modifications to the IC method are proposed in [29–36] to extract GMPP of the photovoltaic

system under PSCs. In reference [37], a comfortable and rapid convergence MPPT method has been suggested, which does not require additional control loops or intermittent links. The algorithm uses the relationship between the load line and the I-V curve and combines with the triangle rule to respond quickly.

To solve the problems mentioned above, artificial intelligence techniques or soft computing techniques have attracted much interest during previous periods, and the MPPT controller's combination enhances its performance to a great extent. Several MPPT controllers based on soft computing algorithms are reviewed in the literature to extract maximum solar power efficiently. Relatively, few papers use the artificial neural network (ANN) to track the solar system's global peak under different shadow conditions. Such as the Artificial Neural Network in [38] and [39] proposed a maximum power point optimization system of the solar system based on polarity information based on neural network and fuzzy logic. The three-layer feed-forward neural network has trained well to find out the maximum global voltage under different shadow conditions. A fuzzy controller based on polarity information is used to obtain the control signal required by the DC-DC converter with the maximum global voltage as the reference voltage. Another purpose of this study is to use the same artificial neural network design to estimate the photovoltaic array's maximum power and energy generation.

In [40], firstly have discussed using Fuzzy Logic Control and then Genetic Algorithm is applied to increase efficiency. The fuzzy controller has two inputs: error and change in error, and controller output are used to track the MPP and the [41] introduces the design and modeling of MPPT controller based on ANFIS. The design consists of PV module, ANFIS reference model, DC-DC boost converter and fuzzy logic (FL) power controller. A new algorithm combining two or more kinds of maximum power point tracking (MPPT) technology is proposed to improve the output DC power and efficiency of photovoltaic array. The first combination is to combine two classical MPPT methods, namely incremental conductance method (Inc) and perturbation observation method (P & O). The second example is the combination of artificial neural network (ANN) and fuzzy logic control (FLC) MPPT based on artificial intelligence. The algorithm is applied to a photovoltaic grid connected system model, and the simulation results show that the algorithm can obtain better static and dynamic response than single MPPT method [42].

Moreover, a Genetic algorithm is applied to improve the result of FLC. In [43], the hybrid genetic algorithm adaptive particle swarm optimization (GAAPSO) method has been used to study the optimal MPPT regulator of multiple photovoltaic panels under partial shading. In this technique, genetic algorithm (GA) and adaptive particle swarm optimization (APSO) are combined to find and capture the global peak (GP) in the local peak (LP) under any conditions. GAAPSO technology has a high tracking speed and higher efficiency than the P & O method. The results show that under the condition of partial shadow, the P & O method cannot track the MPP-GAAPSO method quickly. A direct MPPT method using Fibonacci line search was observed in reference [44]. In this method, the research limit repeatedly moved to include the best advantage in the search limit, which can track the MPP under uniform illumination or smooth change. However, it is relatively difficult to extract the global peak under local shading and harsh environmental conditions. An ANFIS controller for a photovoltaic solar system is proposed in [45]. The system supplies DC power to the load through a DC-DC boost converter. According to climate data such as solar radiation and solar cell temperature, the ANFIS method determines the boost converter's duty cycle. It obtains the MPP of the photovoltaic solar system.

Although this soft computing (SC) technologies are flexible, they are usually more complex and slower than traditional methods. For example, artificial neural networks require precise and extended training cycles to produce accurate results. Also, artificial neural networks need to be implemented by expensive microprocessors because of its computationally intensive nature. On the other hand, FLC shows excellent convergence speed, but its performance depends on the programmer's experience and understanding of specific PV modules and system installation's environmental conditions. Other algorithms such as GA and ACO are also used, but they are mainly used as the optimizer of traditional MPPT; this method is often called hybrid MPPT. Also, in recent years, evolutionary algorithms such as multiverse optimization (MVO) [46], improved multi-universe optimization (IMVO) [47], particle swarm optimization (PSO) [48,49], and grey wolf optimization (GWO) [50] have become good choices for developing MPPT controllers. The metaheuristic algorithm has a fast convergence speed, reduces steady-state oscillation, and is easy to track the maximum global power.

3 The Equivalent Model of Photovoltaic Arrays under the Conditions of Partial Shading

The primary function of photovoltaic systems is to generate energy straight from the sunshine falling on it. Therefore, the PV system is considered a static electricity generator. The central part of the PV system behind generating the electricity from sunlight is the PV cells. The PV cells are probably composed together to form panels or arrays. There are a voltage and current in the terminals of photovoltaic panels that may directly feed small loads like lighting systems and DC motors. Photovoltaic systems come in a range of sizes and outputs appropriate for various applications. They are lightweight, allowing for easy and

safe transportation. These converters may adjust the voltage and current at the load, control the power flow in grid-connected systems, and fundamentally track the GMPP of the photovoltaic systems [51].

PV solar cells are the main-compartment of solar power generation. The PN junction causes to generate solar photovoltaic effect and convert solar energy into electricity. The output power amount of just one single photovoltaic cell is small. The desired power can be achieved in actual applications once forming the photovoltaic array either by string or parallel connection. The output attributes of photovoltaic arrays have characteristics such as nonlinearity and time-variation, which are easily affected by the incident light irradiation intensity, battery body temperature, load conditions, and parasitic impedance, resulting in that the solar energy utilization rate cannot always be maximized. When the solar array is not uniformly illuminated, such as shadows of surrounding buildings, leaves, clouds, etc., the shielded portions cannot be irradiated with regular sunlight, resulting in a smaller current than other non-shaded photovoltaic cells. The current, which becomes a load in the circuit, consumes power, causing the overall output energy to decrease, even causing damage to the photovoltaic cells. At this point, the solar array's output features are more complex, and there may be more than one peak point. Therefore, to better control the photovoltaic power generation system, it is excellent to study the photovoltaic array's output features under the condition of partial shading. This section will set up a mathematical prototype for photovoltaic arrays under the condition of partial shading, combining actual shading conditions with existing photovoltaic cell models.

3.1 Mathematical Prototype of PV Array under the Conditions of Partial Shading

Partial shading is considered one of the main reasons which affect PV curve characteristics. Once the PV system is exposed to abnormal environmental circumstances, particularly the partially shaded case, the nonlinear characteristics of PV curves will get more complicated with several peak maximum power points. Partial shading conditions occur due to many reasons, such as an object covering some parts of the PV arrays for some time, dirt causing a portion of the PV arrays, the clouds covering the sun lights, etc.

The effects of partial shading lead to an increase in the problems in the area of MPPT. When a PV system composes a large number of PV arrays, it is tough to guarantee that each panel receives a similar radiation level. Some of these panels will be exposed to some hard factors such as dust, clouds, trees, etc. will, in practice, be subjected to different amounts of insolation [52]. This phenomenon is called partial shading and can increase complicated I-V and P-V features such as multiplicity of power peaks as seen in Figure 1, which displays local maximum power points (LMPP) and the global maximum power point (GMPP). This puts an exhausting request on the MPPT requirements, as it has to distinguish between local and global maximum power points.

The required voltage and current rating can be satisfied by constructing the PV array using various series and parallel modules. The PV module's protection from the hot-spot problem's adverse effects can be satisfied by connecting each module with a bypass diode, as shown in Figure 1. Furthermore, to guard PV modules against the impact of a potential difference between series-connected strings, each PV string is contacted with a series-connected blocking diode. When the PV array absorbs a similar irradiation level, there will be only one MPP on the PV curve. The PV curve can consist of several local MPP under partial shading case, as shown in Figure 1.

Figure 1 presents a photovoltaic array composed of four modules and its characteristic curves under partial shading conditions. According to the curves, there is three of maximum power point on the curves. However, only one of them is the global maximum power point GMPP.

3.2 Photovoltaic Cell Mathematical Modeling

In order to mathematically establish modeling of the PV array under partial shading, the photovoltaic cell is referred to as (the type of cell construction) a monomer in this paper, as shown in Figure 2(a). Multiple PV cells connected in series and having the same light intensity are called sub-strings, as shown in Figure 2(b); single arrays connected in parallel under the same shading conditions are called sub-arrays, as shown in Figure 2(c). Single cells may be subject to the following three shadow conditions, as shown in Figure 3(a), (b), (c): The first type is the single unshaded cell; the second category is partially shaded single cell; the third category fully shaded single cell.

The shading can be caused by different factors such as surrounding buildings, leaves, clouds, etc. However, the PV cell dimension in the commonly used photovoltaic array is 125mm*125mm. Therefore, the probability of three different intensity lights appearing when a single cell is blocked is tiny. In this paper, there is a maximum of two kinds of light intensity on a single photovoltaic cell, and based on this modeling, most shading conditions can be included.

Once some of the monomers in the PV array are blocked, resulting in non-uniform illumination, the shaded cells act as a load and generate some heat, which may cause a hot-spot effect. This reverse leakage occurs when the two ends are subjected

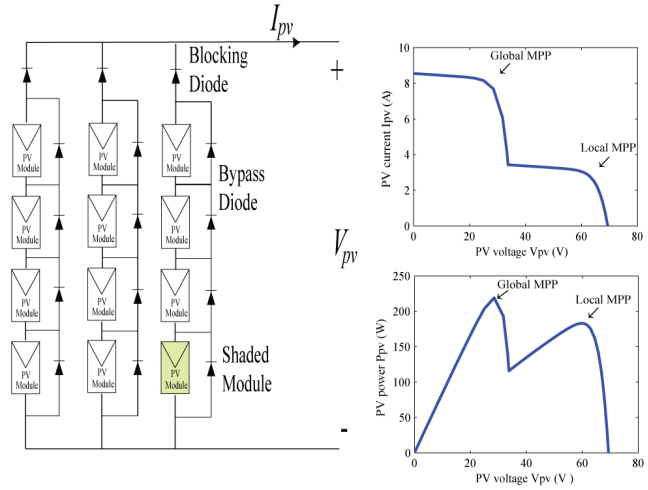

Fig 1. IV and PV curves under partial shading conditions.

to negative pressure to a certain extent, breaking down and damaging the cell. Bypass diodes are used to avoid the hot spot effect and increase the output power of the PV array under partial shading conditions. When the PV array operates under uniform irradiation conditions, all PV cells usually work, and the bypass diode will be in the reverse cut-off state. When a PV cell is shaded, its photon current is reduced, and the voltage drop is negative. At this time, the bypass diode conducts to be like a short-circuit to prevent it from being reversed by the reverse leakage current and increasing the overall output power. The connection of blocking diodes ensures each sub-string direction's direction and prevents each sub-string from affecting each other due to different output voltages. The structure of the PV array with the connection of bypass diodes and blocking diodes is shown in Figure 4.

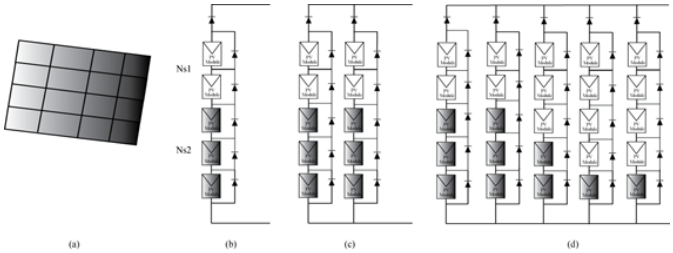

Fig 2. Layout diagram of the PV array.

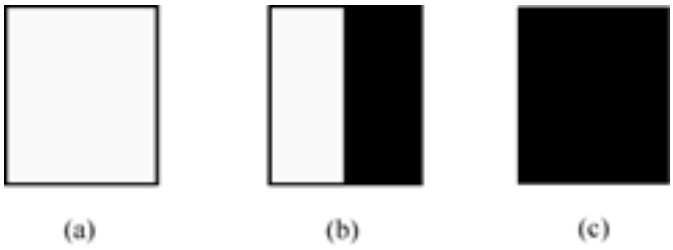

Fig 3. Possible shading distributions on a single PV cell.

In this case, Normal equation cannot be implemented entirely, and the mathematical model of the PV array needs to be modified and re-established. In this paper, the rate of the optical shading E is introduced to indicate the degree of light shading

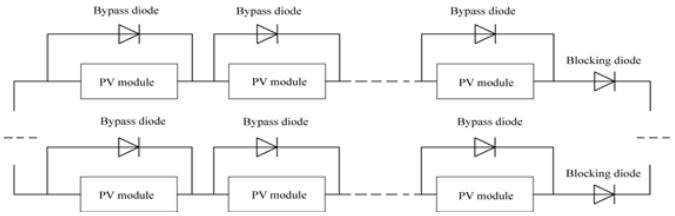

Fig 4. Bypass and blocking diodes configuration of PV array

and the area of the PV array as follows:

$$E = 1 - \frac{G_{\text{after}}}{G_{\text{before}}} \tag{1}$$

Where G_{After} is the solar irradiation received by the PV cell after it being blocked, and G_{before} is the solar irradiation received before the PV cell being blocked. For more straightforward calculation, G_{before} is taken as reference irradiation, which is equal to 1000 W/m^2. The photon current becomes as the following:

$$I_{ph} = I_{ph_0}(1 - E) \tag{2}$$

where I_{pho} is the photon generated current at typical test condition (TTC), 1000 W/m^2 and 25C^o.

As shown in Figure 5, an example of a single string array consists of two photovoltaic cells that are wired in series is studied. In this example, one cell is shaded while the other is not. Therefore both of the photon and output currents of the shaded cell are less than the unshaded cell as I_{pha}<I_{phb}, and I_a< I_b. Also, the specific operation modes have the following conditions:

1. When R_L is relatively large, and the load current $I_L \leq I_a$, then both cell and cell b can work typically and provide the output current. The output voltage and power are the summations of the output voltage and power of each cell.
2. When R_L is relatively small, and the load current $I_L > I_a$, then cell a will be short-circuited by the diode Da and will not provide the corresponding current. The output current and power of the array will be only provided by cell b.

The mathematical model corresponding to this case can be expressed as the following segment function:

$$I_L = \begin{cases} I_{pha} - I_{\circ}\left[e^{\dfrac{q(V_L + 2I_L R_s)}{2AKT}} - 1\right] & \text{If} \quad 0 < I_L \leq I_a \\ I_{phb} - I_{\circ}\left[e^{\dfrac{q(V_L + I_L R_s)}{AKT}} - 1\right] & If \quad I_a < I_L \leq I_b \end{cases} \tag{3}$$

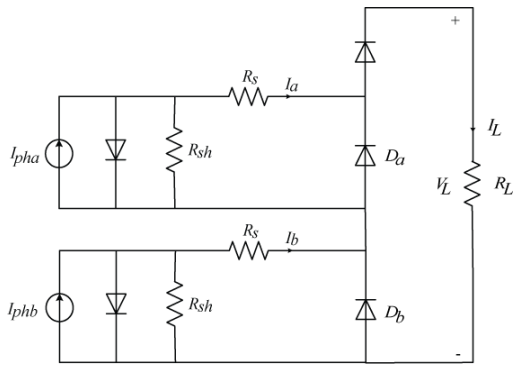

Fig 5. Equivalent circuit diagram of two PV modules connected in series.

The output characteristics of the equivalent model of the PV circuit, which is established by the above Equation, are shown in Figure 6 :

The output current of each PV module, which consists of Ns cells under partially shaded condition, is I_a, I_b, I_c ..... I_{Ns} respectively and each photon current is represented as $I_{pha} < I_{phb} < I_{phc} < ..... < I_{phNs}$ in the following output characteristic equation:

$$I_L = \begin{cases} I_{pha} - I_\circ \left[e^{\frac{q(V_L + N_s I_L R_s)}{N_s AKT}} - 1 \right] & \text{If} \quad 0 < I_L \leq I_a \\ I_{phb} - I_\circ \left[e^{\frac{q(V_L + (N_s - 1) I_L R_s)}{(N_s - 1) AKT}} - 1 \right] & \text{If} \quad I_a < I_L \leq I_b \\ I_{phN_s} - I_\circ \left[e^{\frac{q(V_L + I_L R_s)}{AKT}} - 1 \right] & \text{If} \quad I_{(N_s - 1)} < I_L \leq I_{N_s} \end{cases} \tag{4}$$

When N_P considered being connected with the array structure in parallel, the output characteristics can obtain as the following:

$$\begin{cases} I_L = \sum_{x=1}^{N_p} I_x \\ V_L = \max\{V_x\} \quad x = 1, 2, \ldots, N_p \end{cases} \tag{5}$$

Where I_x and V_x are the output current and voltage of a single string array, respectively.

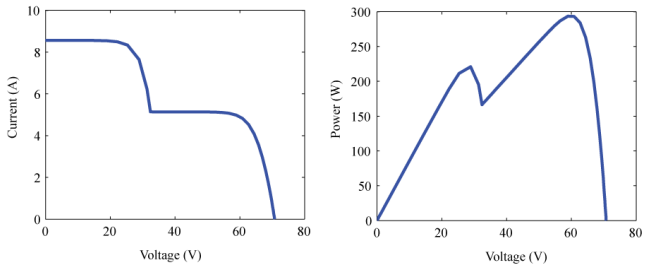

Fig 6. Output characteristics curve under partial shading conditions.

4 DC-DC Boost Converter

The block diagram in Figure 7 shows the essential components of the Boost converter. The boost converter has applications that required stepping up the input voltage to a higher level. The voltage ratio can be calculated, as shown in (9):

$$\frac{V_o}{V_{in}} = \frac{1}{1 - D} \tag{6}$$

The duty cycle D in (6) varies between 0 and 1. That means the voltage ratio is greater than 1, which causes the converter to be used as a step-up converter. The relationship between voltage ratio and duty cycle D is shown in Figure 8 which shows the nonlinearity of voltage ratio and duty cycle relationship of Boost converter. According to this relationship, the voltage ratio change can be significant due to changes in the duty cycle once the voltage ratio becomes high [53].

5 Maximum Power Point Tracking Control Algorithms

A PV array has a nonlinear feature, and its output power relies primarily on the radiation level and the operating temperature. Furthermore, a PV panel's output power is a function of its terminal voltage under the same temperature and irradiance. For all specific PV panels, there is only one value for the terminal voltage that corresponds to the maximum output power. Moreover, to get that voltage, there is a procedure known as maximum power point tracking MPPT. MPPT methods of a PV array could be obtained in two steps, either a single step or a double step. In the case of a single step, a DC/AC converter is utilized. While in the case of double-step, a DC/DC and DC/AC converters are utilized. According to Thevenin's theory, when the value of the power supply's output impedance equals the load, the output will reach the maximum value. Therefore, it is necessary to add an

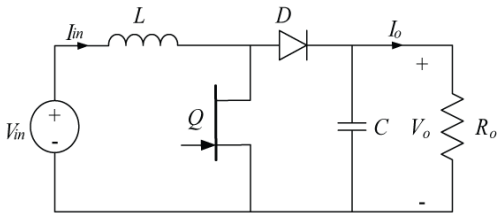

Fig 7. Boost converter circuit [13,54].

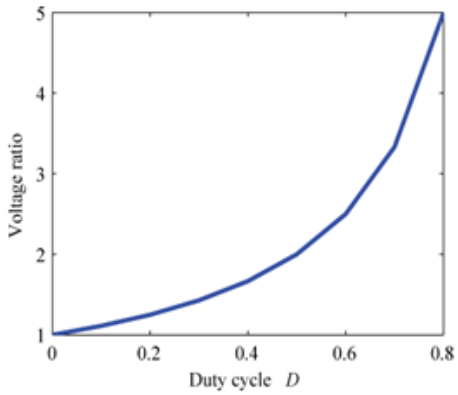

Fig 8. Relationship between duty cycle and voltage ratio of Boost converter.

impedance transformation circuit in the MPPT control system, making the power supply and load reach the state of impedance matching and adjust the output power [55]. The MPPT control system is an essential link in the photovoltaic power generation system; therefore, many practical MPPT algorithms have been applied on different occasions.

The tracking and finding the new altered maximum power point (MPP) in its matching PV solar system curve under any changing radiation level and ambient temperature is the primary duty of maximum power point tracking methods (MPPT). Moreover, it is utilized to catching and given the maximum power from the PV panels and moving that power to the load. A DC/DC (boost/buck) converter performs as linking the PV modules and the load. The MPPT is altering the duty cycle to preserve the transfer power from the PV array to the load at the maximum power point [56–58]. An MPPT control system is an essential link in the photovoltaic power generation system; therefore, many practical MPPT algorithms have been reported on different occasions. This paper will present the MPPT methods based on Cuckoo Search Algorithm (CSA) in detail, compare them with other MPPT methods, analyze their features and drawbacks and related situations, and validate their tracking impact through simulation experiments.

5.1 MPPT based on Artificial Neural Network

Currently, ANN has been enormously advanced in our scientist life, especially in the practical disciplines or the theoretical disciplines, to give us solutions for many complicated tasks. ANN contains three layers: the input layer and the output layer, and only these two layers can connect to the perimeter outside the network. In addition to these two layers, the network contains at least one layer called Hidden Layer because it is not connected to the network's outer perimeter and is only related to the layer that precedes it [59], as known in Figure 9. According to the MPPT field, some parameters can train artificial neural networks like the solar radiation and cell temperature or voltage and current of PV array and any combination of those parameters.

In this paper, the training data which have been collected for training ANN are PV system voltage Vpv, PV system current Ipv, and duty cycle D as seen in Figure 10. The input layer obtains the neural network's input data, propagates it to the hidden layer neurons, and then multiplies it with the weight vector. After multiplication, the output layer reaches the final ANN output. The hidden layer performs the intermediate calculation of the artificial neural network from the input layer to the output layer. The number of neurons in the input layer and the output layer depends on the number of problem inputs and outputs. In contrast, the number of neurons in the hidden layer depends on the required accuracy and calculation time.

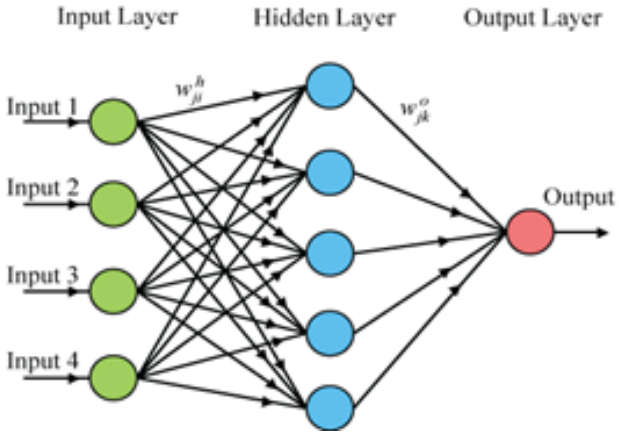

Fig 9. ANN structure for a two inputs-one output system [13].

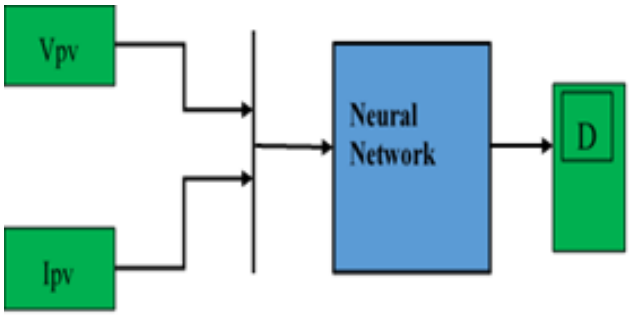

Fig 10. ANN schematic diagram [13].

5.2 Modified of the conventional P&O algorithm

The proposed modification can eliminate the problems of the traditional algorithm. The modified algorithm proposed that the search space is limited to 10% of the power curve, which shortens the response time and reduces the steady-state oscillation,[60,61] pointed out that Vmpp is about 76% of open-circuit voltage (Vmpp = 76% of VOC). Therefore, the P-V curve is divided into three regions, region 1, region 2, and region 3, as shown in Figure 12. Table 1 shows the specifications for each zone. Regions 1 and 3 contain 90% of the power curve area that has been excluded from the search space. Region 2 is the region containing MPP, which is only 10% of the PV curve. The improved algorithm only needs to search the maximum power point in region 2, thus reducing the step response time and eliminating the MPP's steady-state oscillation [62].

Firstly, the voltage V1 and V2 are measured to discover the MPP area. The solar panel's working point is limited to 10% area 2 of the power curve, and then Perturbation and observation are started. MPP is realized and maintained in less perturbation. In uniform weather conditions, it will sustain at the maximum power point. The change of irradiance will find a new local maximum in the same way as the constant irradiance and remain unchanged [62]. Figure 11 shows the flowchart of the modified of the conventional P&O algorithm.

Table 1. Area distribution of power curve.

Regions	Starting (% of Voc)	Ending (% of Voc)	Total area (% of Voc)
Region 1	0	70	70
Region 2	70	80	10
Region 3	80	100	20

Fig 11. Flowchart of the Modified of the conventional P&O algorithm.

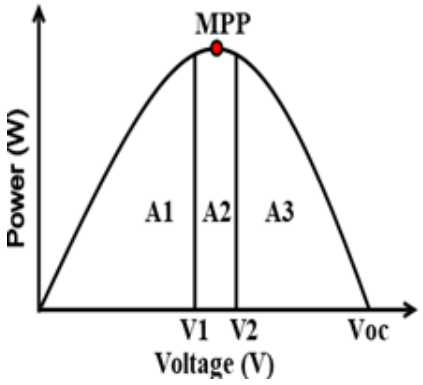

Fig 12. Search space limitation of the power curve.

5.3 MPPT based on Particle Swarm Optimization (PSO)

Particle swarm optimization (PSO) is a search method based on an improved population randomization algorithm. It can reserve the population of each particle to represent the candidate solution. The position expresses the ideal solution to the problem in the optimal particle space. The particle's velocity vector determines the direction and velocity value of the particle. Each particle obeys the current optimal particle and searches for the solution region's optimal solution according to its own flight experience[63–65]. Although the particle swarm optimization algorithm has the advantages of robustness, flexibility, and rapidity, it is easy to fall into local optimization in the tracking process and not reach the global peak.

5.3.1 Modified Particle Swarm Optimization (MPSO)

In the typical particle swarm optimization algorithm, the "particle" part refers to the population members with small mass and small volume affected by speed or acceleration and with the best performance. Each particle in the swarm represents a solution in a high-dimensional space. The four vectors are: 1) current position; 2) unique optimal position of all particles after accelerating relative to the old position; 3) particle velocity; and 4) global optimal position of all particles originated from its neighborhood so far. Each particle adjusts its position X_{ij} in the limited search area according to its best position $X_{Pbest.ij}$, All the particles are in the best position $X_{Gbest.ij}$ as seen in Figure 13 . The following formula can be used through the optimal search process to explain in detail[54].

The first modification is the velocity step function V_{ij}^{t}Adopted by the classical particle swarm optimization algorithm. It is determined for each particle ith of each jth variable in each iteration t, where $V_{ij}^{t} \geq 0$, as shown in Equation (7), it is a three-part equation. Three average values fix the particle, and the inertia function ω can be calculated in each iteration of formula (8); the limit value of inertia operator and the third term are the maximum number of fitting iterations t_{max}; the second item is the

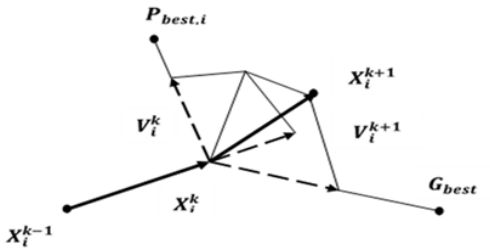

Fig 13. Movement of a particle in the optimization process

program of updating the current position. The third item is updating the current position, indicating that the global best solution is shared between the old positions Case information method. Here, a significant change is that global optimization should also guide the individual optimal solution as the convergence process's acceleration factor, which can be expressed mathematically by formula (9). Therefore, the other two changes made to the old velocity function are c1, c2, c3, and c4, which are called constant parameters and random numbers of MPSO, r1, r2, r3 r4, which are between [0,1].

$$V_{ij}^{t+1} = \omega V_{ij}^{t} + c_1 r_1 \left(X_{Pbesi\ j}^{t} - X_{ij}^{t} \right) + c_2 r_2 \left(X_{\text{Gret.}\ i}^{t} - X_{ij}^{t} \right) \tag{7}$$

$$\omega^{t} = \omega_{\max} - \left(\left(\omega_{\max} - \omega_{\min} \right) / t_{\max} \right) \times t \forall \omega \geq 0 \tag{8}$$

$$V_{ij}^{t+1} = V_{ij}^{t+1} + c_3 r_3 \left(X_{Gtett,j}^{t} + X_{Pbeti\ j}^{t} - 2X_{ij}^{t} \right) + c_4 r_4 \left(X_{\text{Glest}\ ,i}^{t} - X_{Pbeti\ j}^{t} \right) \tag{9}$$

The second modification is updating the i_{th} particle location which Any particle should pass the step function V_{ij}^{t} appropriately updates its position to move to the optimal state, as shown in Equation (10), where a step is added to the current position, which may be positive or negative until it becomes zero, then it is the optimal solution:

$$X_{ij}^{t+1} = X_{ij}^{t} + V_{ij}^{t+1} \tag{10}$$

We can consider narrowing the search area to find that the optimal value is another modification to the search process. It needs to adjust and modify the restrictions of control variables in each iteration. Therefore, for X_i the limit of the control variable is reduced to converge to the optimal global position in each iteration compared to its old limit. Therefore, the limit reduction strategy can be proposed by using mathematical equations. In (11) and (12), σ is the coefficient of less than 0.1, randomly selected and adjusted according to the problem.

$$X_{i,\max}^{t+1} = X_{i,\max}^{t} - \sigma \left(X_{i\max}^{t} - X_{\text{Gbest}\ 1}^{t} \right) \tag{11}$$

$$X_{i,\min}^{t+1} = X_{i,\min}^{t} - \sigma \left(X_{Gbest.i}^{t} - X_{i,\min}^{t} \right) \tag{12}$$

The last modification is that the speed step or step size is based on the maximum/minimum value x of the controlled variables X_j^{max}, X_j^{min} This is very beneficial to obtain the optimal solution. The speed limit V_j^{limits} limits can be modified according to each situation or system, and the value of speed limit operator β can be appropriately selected, as shown in Equation (13)

$$V_i^{\text{limits}} = \pm\beta \left(X_i^{\max} - X_i^{\min} \right) \tag{13}$$

This section shows how optimization deals with the difficulties of photovoltaic systems. The complex control variables, objective functions and system constraints of the photovoltaic system are defined. The above optimization techniques are now implemented on the MPPT controller of the PV system under consideration, which operates under the PSC. Figure 14 shows a flowchart of the complete implementation of the proposed work using MPSO. Here, the particle's position is used as the duty cycle (D) of the converter, and the fitness value of the particle is the P_{PV} power produced by the whole photovoltaic system.

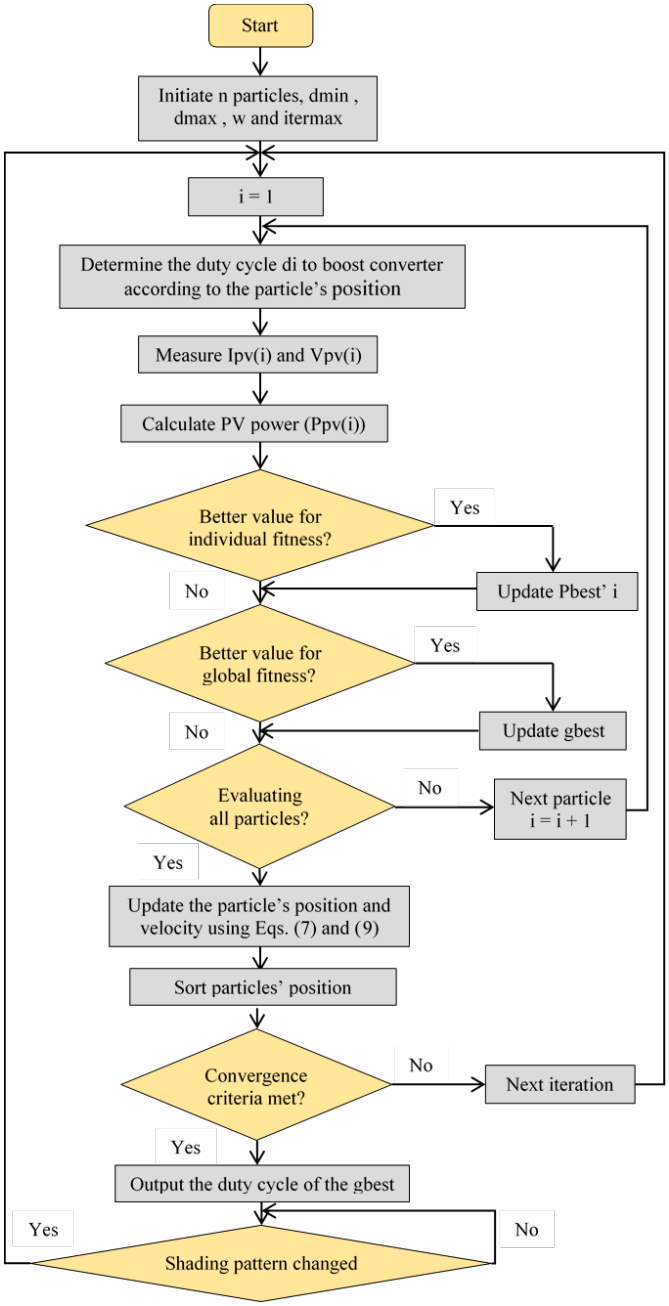

Fig 14. Modified particle swarm optimization process flowchart

5.4 MPPT based on Cuckoo Search Algorithm (CSA)

In recent years, many evolutionary algorithms based on natural metaheuristics algorithms have been improved in optimization. These algorithms usually work in suitable search areas based on a random search, which depend on or optimize complex problems. However, there will also be many mechanisms to lead the search so that the solution vector will progress with the number of iterations, so the search is not random. The intensive (Development) and diversified (exploration) are the two essential features of these recent metaheuristic algorithms.

5.4.1 Cuckoo's Behavior

In 2009, Yang and Deb were proposed a natural optimization algorithm CSA. This is a new metaheuristic algorithm, which has already been applied in many optimization types of the research area. Also, CSA's inspiration comes from cuckoo chicks' parasitic behavior, which has a robust reproductive ability when laying eggs in the host nest. Therefore, the determination of egg-laying and body shape breeding of cuckoo is based on the optimization algorithm. There are two formulations of cuckoo in the optimization process: egg and mature cuckoo. If adult cuckoos lay eggs in their nests and the host bird does not find or kill the eggs, they will grow into mature cuckoos. The cuckoo community's environmental characteristics and migration help the cuckoo gather and find the best habitat for breeding. This optimal residential area is the global maximum of the objective function [(66)].

Cuckoos are fascinating because they make beautiful sounds, and because of their breeding strategies. Some of the cuckoo's species, such as Killa and Anne, are laying their eggs in community nests and eliminating other birds' eggs to progress their chances of hatching their eggs. Some cuckoos lay eggs and parasitize only in host bird's nests. There are three basic types of parasitism: intraspecific parasitism, cooperative propagation, and nest attachment. Several host birds clashed directly with the parasitic cuckoo. If the host bird gets the cuckoo's eggs, immediately, it will throw them away or leave its nest and build a new one in another place. Some cuckoo species have evolved so that the female parasite mimics the color and shape of the eggs of a few selected host species. This increases the possibility of eggs hatching, thus improving their reproductive capacity.

5.4.2 Levy Flight Mechanism

The most critical part of the cuckoo breeding strategy is to find a convenient host nest. In general, looking for a nest is similar to looking for food, and it takes the form of random or quasi-random. Generally speaking, when animals are looking for food, they will choose the direction or track simulated by a specific mathematical function. One of the most common modes is Levy flight. Levy flight can be regarded as a random walk, in which step size has a levy probability distribution. In cuckoo bird search, birds nest search is characterized by Levy flight. Mathematically speaking, Levy flight is a kind of random walk. According to power law, the step size is extracted from Levy distribution as follows:

$$y = l^{-\lambda} \tag{14}$$

Where is the flight length, and λ is the variance. Because $1 < \lambda < 3$ so y has infinite variance. Figure 15 is an instance of Levi flight in a two-dimensional area. Because of tax distribution advantages, these steps are composed of many small steps and big steps, long-distance jumps. Moreover, compared to other heuristics algorithms, these long-distance jumps can significantly improve the efficiency of cuckoo search, especially for multimodal and nonlinear problems.

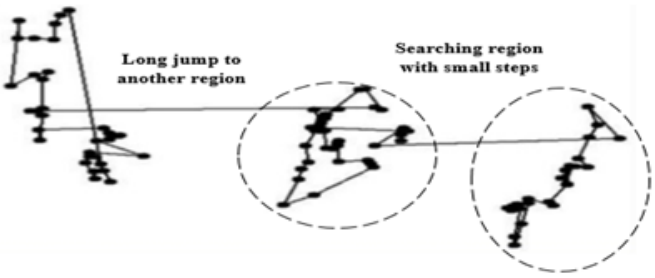

Fig 15. Levy Flight in a two-dimensional Plane

5.4.3 Method of Optimization

The algorithm starts with a premier population of cuckoos. The original cuckoo laid its eggs in the host bird's nest. Therefore, some of the eggs that have more similarity to the host birds' eggs will grow and hatch into mature cuckoos. Other eggs found by the host birds were destroyed. Mature eggs can detect the quality of nests in that area. The more eggs a region has, the more profits it makes. Therefore, the term CSA is going to optimize will be where more eggs survive [(66)].

To improve the rate of still alive for cuckoo eggs, cuckoo should look for the rightest area to lay eggs. When the remainder of the eggs grows into mature cuckoos, they will make some societies. Every society has its environment area to live and reproduce. The best environment for all societies will be the aim of other societies. Then cuckoos migrate to their best environments. They will live close to the best habitat [(66)].

5.4.4 Cuckoo Search via Levy Flights

Affording to the nest parasitism actions of cuckoo birds, CSA has three idealized rules: 1) Each cuckoo lay one egg at a time and then put it inside a randomly selected nest; 2) the nest with the best quality of getting chance of surviving of the cuckoo will be moved to the following generation; 3) the number of nests available is fixed, and the probability of keeping cuckoo eggs distinguished by host birds is Pa, of which $0 < Pa < 1$.

For the maximization problem, the value of the objective function can be directly proportional to the solution's fitness. For simplicity, we can use the symbol: all eggs in a nest characterize a solution, and cuckoo eggs characterize a new solution. The aim is to use new and potentially better solutions (such as cuckoo) instead of less reasonable solutions in the nest. If a cuckoo's egg is detected, the host bird can leave its nest or destroy the cuckoo's egg. On the other hand, if the numeral of nests is fixed, the new nests will be built by Pa's probability.

When a new solution is generated for cuckoo, Levy flight will be performed according to the next expression

$$X_i^{t+1} = X_i^t + \alpha \oplus \text{Levy}(\lambda) \tag{15}$$

Where X_i^t is the sample/egg, i is the number of samples, t is the number of iterations, and α is the step size related to the scale of the problem of interest. In most cases, we can use $\alpha = 1$, sometimes $\alpha > 0$. The random walk is a Markov chain whose following location relies only on the present position (the first term in the above Equation) and the transfer probability (the second term). Product $\oplus$ means multiplication by entry. In most cases, α is used for the next Equation, that is:

$$\alpha = \alpha_0 \left(X_j^t - X_i^t \right) \tag{16}$$

where α_0 is the primary step size; in this calculation, the change between the two samples is used to fix the subsequent step size. Under the MPPT algorithm background, the structure of CSA in formula (15) is similar to HC / P & O method. Of course, this similarity does not include the step size of the Lévy flight. However, the main advantages of the CSA algorithm are more robust than the HC algorithm: (1) CSA algorithm is a population-based algorithm (such as GA and PSO), but it shows advantages in the selection process (such as harmonious search); (2) CSA algorithm has higher randomization efficiency; because Lévy flight, sometimes the step size becomes larger (long jump), and the convergence speed is faster, (3) There are only two parameters for parameter setting in CSA; GA and PSO need three or more parameters; and (4), unlike PSO, CSA performance does not depend on sample initialization.

5.4.5 MPPT Using CSA

In order to use CSA to design MPPT, it is necessary to select appropriate variables to search. First, in this case, all samples are defined as the value of photovoltaic voltage, i.e., VI (I = 1,2). n). The total number of samples is defined as (n). Secondly, the step size is expressed in (α). Then the fitness function (J) is the photovoltaic power value of the maximum PowerPoint. Because J depends on PV voltage, J= f(V). Initially, the resulting sample is applied to the PV module, and the power is set to the initial adaptation value. The voltage corresponding to the maximum power count is considered to be the largest sample at present. Then, according to the Levy flight executed in the next calculation [67], a new voltage sample is generated accordingly:

$$V_i^{t+1} = V_i^t + \alpha \oplus \text{Levy}(\lambda) \tag{17}$$

where $\alpha = \alpha_0 \left(v_{\text{best}} - v_i \right)$ A simplified structure of the Levy supply can be explained by:

$$s = \alpha_0 \left(v_{\text{best}} - v_i \right) \oplus \text{Levy}(\lambda) \approx K \times \left(\frac{u}{\frac{1}{v}\beta} \right) \left(v_{\text{best}} - v_i \right) \tag{18}$$

here $\beta = 1.5$ is the levy times the coefficient (at the designer's option), while u and v are calculated from the usual distribution curve. Measure the specific power of the new voltage sample from the PV module. The maximum power given by the voltage is selected as the new best sample by comparing the power values. In addition to the best sample, other samples are destroyed at random with a probability of Pa. This process stimulates the host bird's behavior of discovering cuckoo eggs and destroying them. Then a new random sample is generated to replace the broken sample. Therefore, all samples' power is measured again, and the current optimal value is selected by calculating J. The iteration continues until all samples reach MPP.

5.4.6 Flowchart of CSA MPPT

Figure 16 displays the suggested technique's flow chart, initializing all constants and variables, i.e., voltage, current, power, number of samples. Use the current value of voltage and current to compute the power. The new values of voltage and power are deposited in the voltage and fitness arrays, respectively. Besides, before each iteration begins, a check is performed to determine whether the sample has reached convergence or otherwise. If the samples are close to MPP, they will be merged into the same value, and the corresponding power will be merged into the same value[68]. If all samples do not converge, all the corresponding samples' power values are restrained and deposited in the fitness array. By estimating the array, the sample with the immense power is selected as the best sample. After that, all other samples are enforced to keep moving to this optimal value. Performing a Levy flight will then calculate the steps described in equations (17) and (18). Therefore, a new set of samples was found. Then, the corresponding power of these new samples is restrained from the photovoltaic panel. If any sample results in low power, the specific sample is ignored, and a new sample is produced. This iteration will continue until all samples reached the greatest MPP[68].

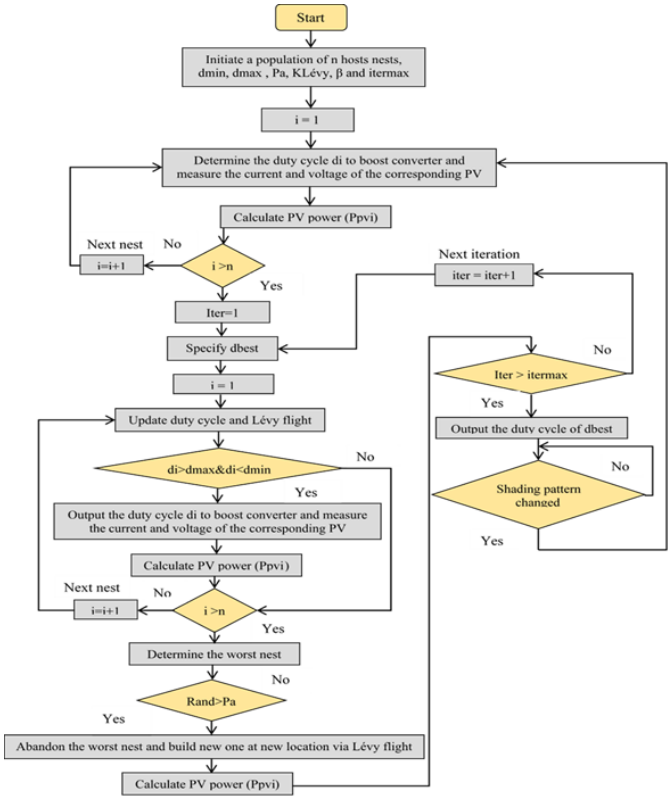

Fig 16. Flowchart of Cuckoo Search Algorithm

In general, under partial shading conditions, when using the method of Cuckoo search to obtain the global peak of maximum power of PV arrays, the search process has to be made by choosing suitable variables. The output voltage and step size are the two parameters of the Cuckoo search algorithm. If the new sample is more than the old sample, then the new sample's maximum power is selected as the new best sample. If the new sample has a lesser amount than the old sample, the maximum power is kept. The course continues until all samples have reached the MPP[7–11].

6 Simulation Results

The previous sections show that the global maximum power point's location depends on two factors; the first factor is how shadow shading is distributed on PV arrays, and the second one is how PV panels expose solar irradiation. As a result, the implementation of traditional maximum power point tracking algorithms to catch the global maximum power point's exact location is exceptionally tricky. Therefore, it is necessary to propose a new method with fast and accurate global search capability and be superior to the traditional MPPT algorithm in dynamic stability performance and other aspects.

This section will show all the simulations for the Photovoltaic array, the boost converter, the proposed artificial cuckoo search algorithm comparing to MPSO, MP&O, and ANN methods. All the simulations are done using MATLAB/SIMULINK software. The simulation results and some case studies for the whole proposed system are discussed in this section.

The schematic diagram of the proposed system, which shows the overall PV system connected to the proposed MPPT predictor, is clarified in Figure 17. It consists of four PV arrays connected in series, MPPT trackers, DC-DC boost converter, and load. The PV experimental platform and control monitoring system used as a reference to design the proposed system is shown in Figures 18 and 19.

For PV array simulation, the simulated PV module has the same parameters as the UP-S250 module at standard test condition (STC), as shown in Table 2 . The PV system has been modeled using MATLAB/Simulink to provide the required output voltage and output currents. The inputs of the PV system are both radiation and temperature. The other parameters have been taken into consideration, as explained before in the equations of PV systems.

Fig 17. Platform of experimental PV lab

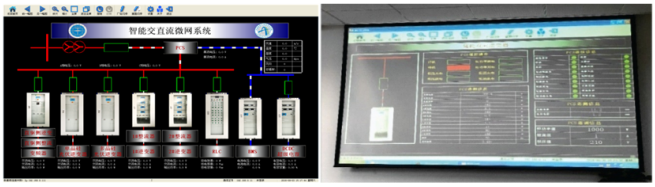

Fig 18. Experimental control monitoring system

Table 2. UP-S250 PV module electrical parameters

Parameters	Values
Maximum Power (P_m)	250 W
Open – circuit Voltage (V_{oc})	36.0 V
Short – circuit Current (I_{sc})	8.56 A
Maximum Power Voltage (V_{mmp})	30.2 V
Maximum Power Current (I_{mmp})	8.28 A
Number of Series Modules (N_s)	4
Number of cells per module N_{cell}	60

6.1 Partial Shading Distribution Scenarios of PV System

The proposed controlling method's effectiveness is investigated by assuming three shading scenarios, and the PV characteristics curves under partially shaded conditions for all scenarios are presented below.

In the first scenario of investigating PSC, the PV system is exposed to three different irradiation levels and PSC (900, 1000, 400, 1000 W/m^2) and one constant level of temperature (25°C). As presented in Figure 20, the PV curve has two local peaks (485.9, 459.6 W) and one global peak (702.136W), located at the second peak of the P-V curve. Figures 21 and 22 show the PV system simulation results (power, voltage, current, and duty cycle of the DC-DC boost converter) obtained from different MPPT techniques under the first partial shading pattern. It presents that the proposed MPPT method based on heuristic algorithms CSA and MPSO can track the actual maximum power efficiently whatever are the shading conditions. CSA-based MPPT method has a better response in waveform harmonics distortion and lower than the MPSO method. The maximum global

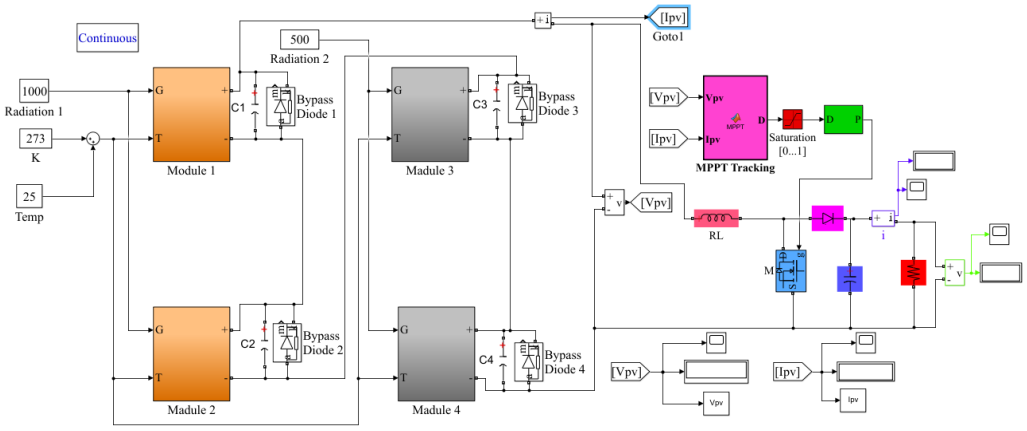

Fig 19. Modeled components of the proposed system.

power is effectively extracted via CSA tracker within a short time and free oscillations compared to MPSO, MP&O, and ANN method. CSA and MPSO methods track the GMPP in 0.55s and 2.8s, respectively. However, MP&O and ANN methods cannot track the GMPP and are trapped at the P-V curve's first peak.

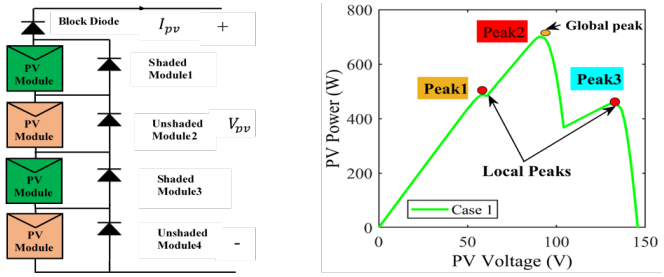

Fig 20. PV characteristics curve and Shading patterns for scenario one.

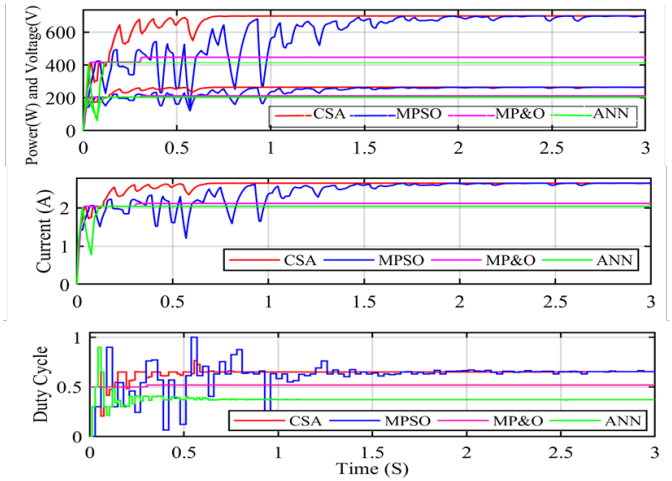

Fig 21. The output Power, voltage current, and duty cycle comparison between the CSA and different methods at the first scenario of PSCs.

In the second scenario of investigating PSCs, solar radiation is considered (900, 1000, 1000, 900 W/m^2) and one constant temperature (25°C). The P-V curve is shown in Figure 23. In these conditions, the PV curve has one local peak (486.2 W) and one global peak (930.93W), located at the second peak of the P-V curve. CSA and MPSO methods can identify the GMPP

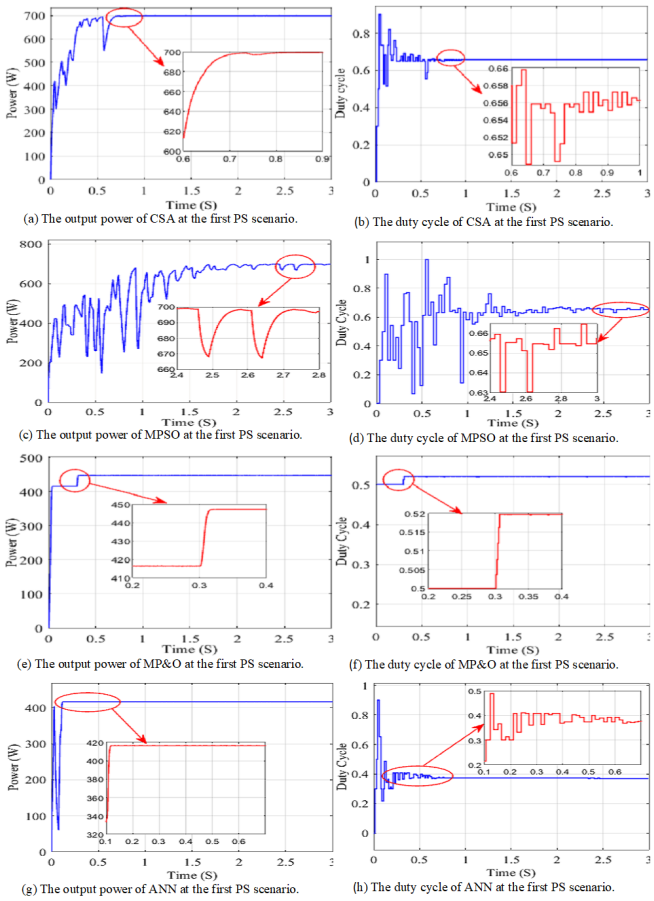

Fig 22. Detailed simulation results of MPPT trackers for PV system under first partial shading (PS) scenario.

and successfully track the global MPP at 0.6s and 2.8s. The MP&O and ANN method have converged when the power value is 764.5W and 717.5W, respectively. Details of the comparison of simulation results are shown in Figures 24 and 25 for various techniques of MPPT under the second pattern of partial shading condition.

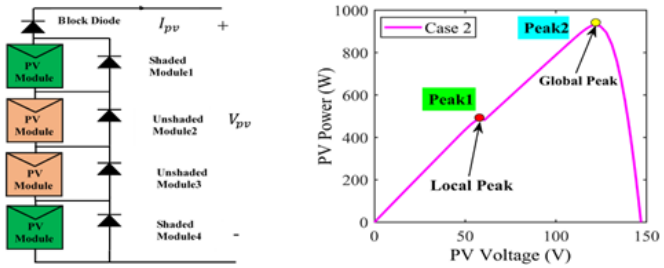

Fig 23. PV characteristics curve and Shading patterns for scenario two

In scenario three, the PV system is exposed to three different irradiation levels (900, 500, 1000, 500 W/m^2) and one constant level of temperature (25C^o). As presented in Figure 26, the PV curve has two local peaks (231.9, 454.5 W) and one global peak (542.606W), located at the third peak of the P-V curve. Figures 27 and 28 compares the performance of various techniques of MPPT subjected to the third pattern of partial shading condition. As expected, both algorithms-being based on search mechanism, can handle the partial shading conditions well. However, CSA is comparatively faster; after the occurrence of partial

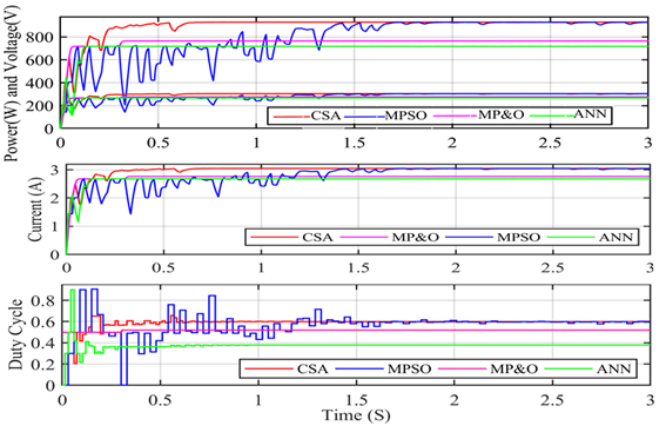

Fig 24. The output Power, voltage current, and duty cycle comparison between the CSA and different methods at the second scenario of PSCs.

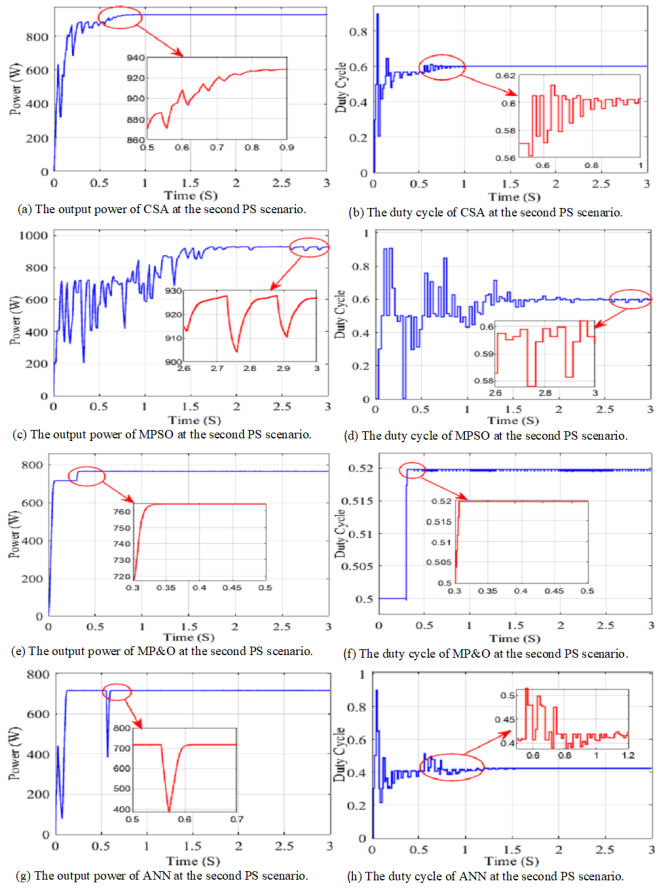

Fig 25. Detailed simulation results of MPPT trackers for PV system at second partial shading (PS) scenario.

shading, CSA tracks the MPP within 0.3s with zero fluctuations in steady or transient states, while MPSO requires 1.7s. Besides, MPSO presents more significant fluctuations in steady or transient states. Also, the MP&O and ANN quickly get trapped at the local peak.

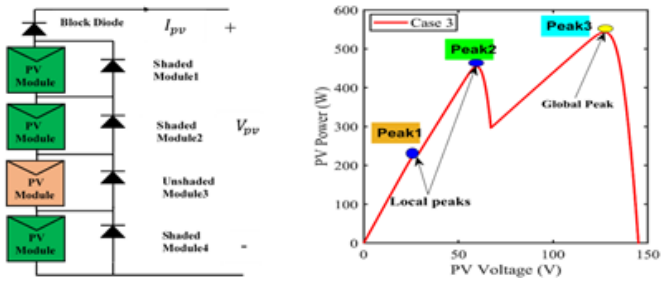

Fig 26. PV characteristics curve and Shading patterns for scenario three.

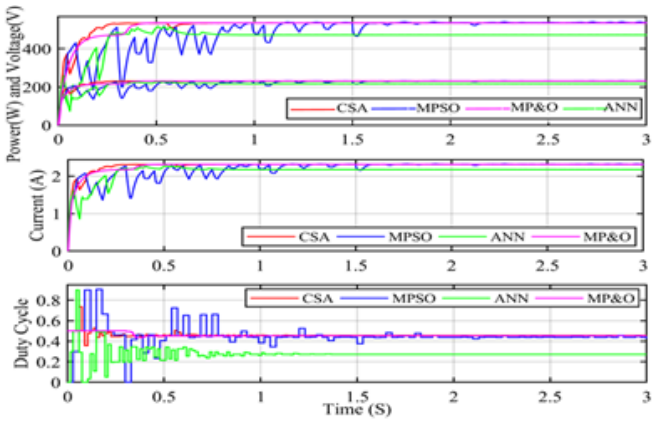

Fig 27. The output Power, voltage current, and duty cycle comparison between the CSA and different methods at the third scenario of PSCs.

In the fourth scenario of investigating PSC, solar radiation is considered (900, 650, 800, 700 W/m^2) and one constant temperature (25C^o). The P-V curve is shown in Figure 29. The PV curve has three local peaks (208.9, 405.5, 557.4 W) and one global peak (701.811W), located at the fourth peak of the P-V curve. Tracking performance of designed MPPT controllers under the fourth pattern is illustrated in Figures 30 and 31 . the conventional MP&O provides power tracking near the GMPP region, which the power of the track is 691.2W, and the ANN MPPT tracks power as 666.6W. On the other hand, MPSO reaches near to GMPP also of 673.2 W whereas CSA MPPT finds the GMPP. Therefore, the CSA is efficiently tracking the location of the global peak within a short time and free oscillations in contrast to other designed MPPT controllers.

Finally, it can be construed that CSA and MPSO algorithms can track the GMPP while the conventional MP&O and ANN always drop to the local peak and the performance of the CSA method is superior to MPSO, MP&O and ANN methods where it converges in a shorter time compared to other designed MPPT controllers. For further study, as it was shown in Figure 32, the output load connected to the PV system is increased from 50 ohms to 120 ohms with steps of 10 ohms, and a comparison is made between CSA, MPSO, P&O, and ANN methods. The solar radiation intensity is considered as 1000, 800, 500, and 900W/m^2, respectively. As shown in Figure 32, the MPSO method has failed to track the maximum power point for 110-ohm load and was trapped in the local optimum. The MP&O method has caught the maximum power point for 50 ohms and 60-ohm load and was trapped in the local optimum in the other loads as well as the ANN controller has achieved the maximum power point for 50 ohms, 60 ohms, and 70-ohm load and was failed in tracking the maximum power point for other loads and trapped in the local optimum. According to this figure, the output load is effective only on the maximum power point location and makes this point to displace. As it is clear from Figure 32, by increasing the load from 50 to 120 ohm, the optimum duty cycle has increased from 0.3279 to 0.6649. The output load only displaces the maximum power point, and the optimization methods are

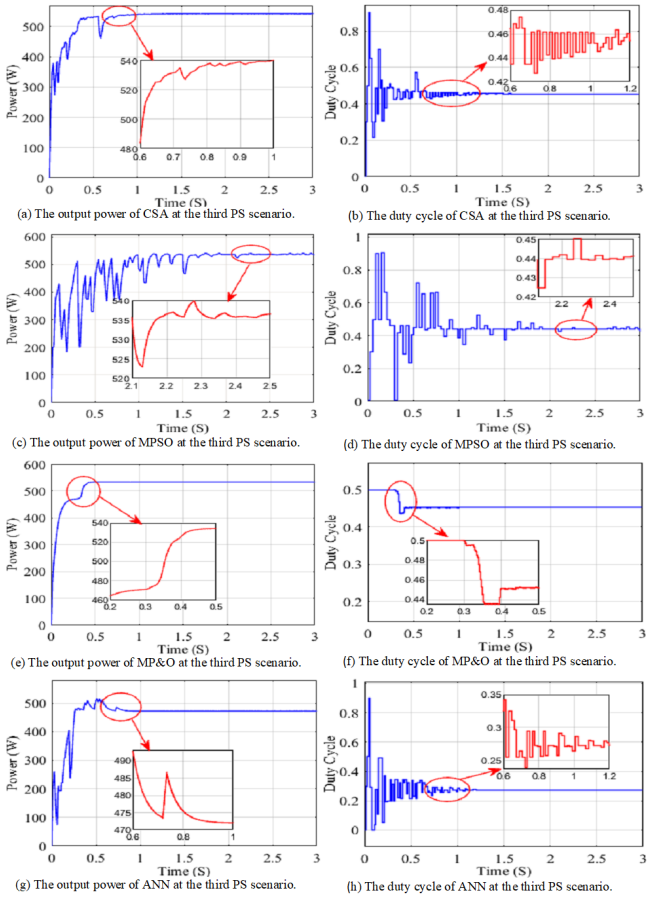

Fig 28. Detailed simulation results of MPPT trackers for PV system under third partial shading (PS) scenario.

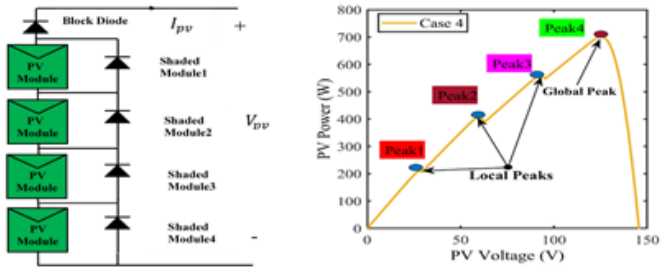

Fig 29. PV characteristics curve and Shading patterns for scenario four.

not affected because of random initialization. The maximum global power is effectively extracted within a short time, which is between (0.2 to 0.5 s) and free oscillations as shown in the above mentions figures, which prove that the proposed method CSA may easily track the global peak without any difficulty.

As mentioned in Tables 3, 4, 5 and 6, the proposed tracking methods can distinguish between the local and global peaks for each scenario. As a result, the system performance has improved, and the proposed trackers' output power values are close to the maximum power.

The proposed MPPT method(CSA) have the ability to track the actual maximum power, whatever are the shading conditions and scenarios. For all considered shading scenarios, it has been noticed that the proposed method can easily track the actual maximum power for the UP-S250 PV array system. As well, under non-uniform irradiation condition and PSCs for all scenarios,

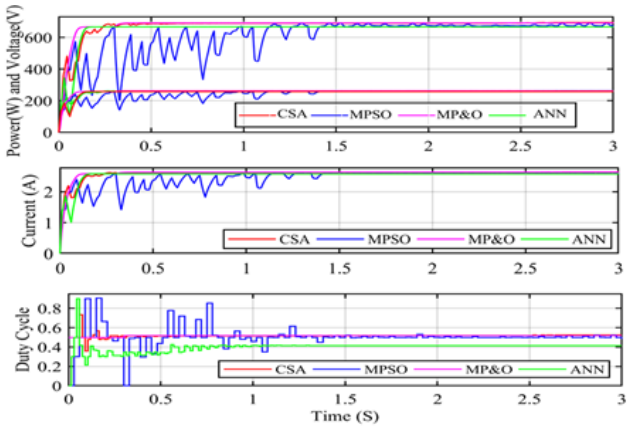

Fig 30. The output Power, voltage current, and duty cycle comparison between the CSA and different methods at the fourth scenario of PSCs.

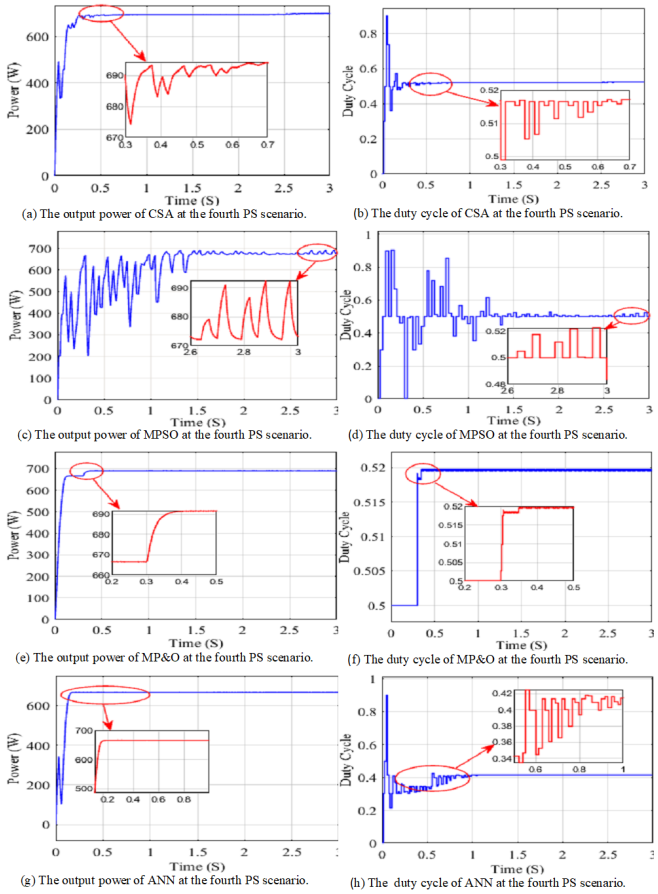

Fig 31. Detailed simulation results of MPPT trackers for PV system at fourth partial shading(PS) scenario.

Table 3. The maximum power point and voltage under different shadow distribution cases

Cases	Radiations (G)				P_{max}	V_{max}
	PV1	PV2	PV3	PV4		
Case 1	900	1000	400	1000	702.136	91.257
Case 2	900	1000	1000	900	930.93	121.518
Case 3	900	500	1000	500	542.606	127.664
Case 4	900	650	800	700	701.811	125.396

Table 4. Power values comparison between (CSA, MPSO, MP&O, and ANN).

Scenario	Pmax (W)	Pmax-CSA (W)	Pmax-MPSO (W)	Pmax-MP&O (W)	Pmax-ANN (W)
Scenario 1	702.136	699.6	699	447.2	416.6
Scenario 2	930.93	928.5	927.1	764.5	717.5
Scenario 3	542.606	534.7	536.2	534.6	472.1
Scenario 4	701.811	694.7	673.2	691.2	666.6

Table 5. Voltage values comparison between (CSA, MPSO, MP&O, and ANN).

Scenario	Vmax (V)	Vmax-CSA (V)	Vmax-MPSO (V)	Vmax-MP&O (V)	Vmax-ANN (V)
Scenario 1	91.257	264.5	264.4	211.5	204.1
Scenario 2	121.518	304.7	304.5	276.5	267.9
Scenario 3	127.664	231.2	231.6	231.2	217.3
Scenario 4	125.396	263.1	259.5	263	258.2

Table 6. Duty cycle values comparison between (CSA, MPSO, MP&O, and ANN).

Scenario	D-CSA	D-MPSO	D-MP&O	D-ANN
Scenario 1	0.6572	0.6576	0.5198	0.3713
Scenario 2	0.5999	0.5963	0.5198	0.3795
Scenario 3	0.4559	0.4277	0.4523	0.2724
Scenario 4	0.5261	0.4834	0.5198	0.4142

it can be showed that the proposed technique shows fast response and good stabilization at the actual maximum Power Point, and the global MPPT can be tracked rapidly with almost 99% efficiency for all investigated scenarios compared to MPSO, MP&O and ANN methods.

6.2 Statistical Evaluation of the Proposed Algorithms

In this section, a descriptive statistical analysis is introduced to evaluate, organize, and summarize the proposed algorithms' results. Moreover, sensitivity analysis is introduced to test the performance stability of these algorithms. The worthy statistical metrics for this evaluation are; the Error, Efficiency, Tracking Time, and Wasted Power. These metrics can be estimated as the following:

$$\text{Error} = \left| \frac{P_{\max} - P_{MPPI}}{P_{MPPT}} \right| \times 100 \tag{22}$$

$$\eta = 1 - \frac{P_{\max}\ \text{actual} - P_{\max} MPPT}{P_{\max}\ \text{actual}} \times 100 \tag{23}$$

Tables 7, 8, 9 and 10 showed that CSA, MPSO, MP&O, and ANN algorithms have a reasonable Tracking time. Furthermore, Error and Efficiency values demonstrated no change of the results over the iterative circle for both CSA and MPSO. Simultaneously, there is a significant change in the results for MP&O and ANN, which proves the proposed algorithms' stability with the priority of the CSA algorithm. The comparison between the statistical results of CSA, MPSO, MP&O, and ANN algorithms are displayed in Table 11 and Figure 33.

Figure 33. Comparison between statistical results of CSA, MPSO, MP&O, and ANN algorithms. Table 11 and Figure 33 showed that CSA retains the least Error compared to other algorithms. However, the Wasted Power value of the CSA algorithm

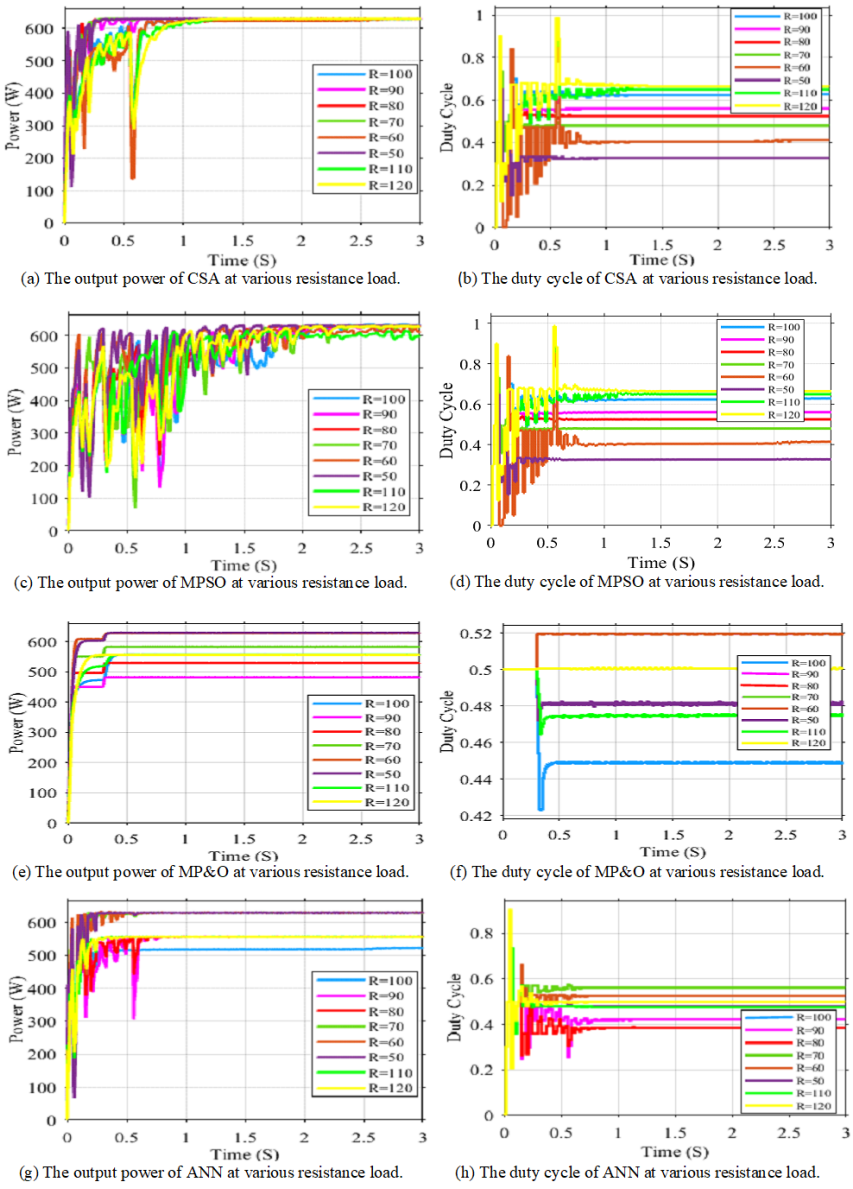

Fig 32. Detailed simulation results of MPPT trackers for PV system under various resistance load.

Table 7. Evaluation of the statistical performance of CSA.

Scenarios	Wasted Power (W)	Tracking Time (s)	Efficiency (η%)	Error (%)
Scenario 1	2.536	0.6	99.64	0.3625
Scenario 2	2.43	0.7	99.74	0.2617
Scenario 3	7.906	0.6	98.54	1.4789
Scenario 4	7.111	0.5	99	1.0236

Table 8. Evaluation of the statistical performance of MPSO.

Scenarios	Wasted Power (W)	Tracking Time (s)	Efficiency (η%)	Error (%)
Scenario 1	3.136	2.7	99.55	0.4486
Scenario 2	3.83	2.9	99.589	0.4131
Scenario 3	6.406	2.4	98.82	1.1947
Scenario 4	28.611	3	96	4.25

Table 9. Evaluation of the statistical performance of MP&O.

Scenarios	Wasted Power (W)	Tracking Time (s)	Efficiency (η%)	Error (%)
Scenario 1	254.94	0.3	63.7	0.4486
Scenario 2	166.43	0.3	82.122	0.4131
Scenario 3	8.006	0.5	98.524	1.1947
Scenario 4	10.611	0.4	98.488	4.25

Table 10. Evaluation of the statistical performance of ANN.

Scenarios	Wasted Power (W)	Tracking Time (s)	Efficiency (η%)	Error (%)
Scenario 1	285.536	0.2	59.333	68.54
Scenario 2	213.43	0.6	77.073	29.746
Scenario 3	70.506	0.7	87.006	14.934
Scenario 4	35.211	0.2	95	5.282

Table 11. Effectiveness comparison between (CSA, MPSO, MP&O, and ANN).

Tracker	Wasted Power(W)	Tracking Time (s)	Efficiency (η%)	Error (%)
CSA	4.312	0.56	99.457	0.576
MPSO	14.562	1.5	98.065	1.973
MP&O	115.562	0.56	84.648	18.136
ANN	126.945	0.9	83.136	20.285

demonstrates its stability compared with MPSO, MP&O, and ANN algorithms, along with all scenarios. Moreover, the Efficiency of CSA is improved to 99.457 concerning MPSO, MP&O, and ANN (98.065, 84.648, and 83.136), respectively. Concerning efficiency, CSA is the superior one in all scenarios, followed by MPSO and MP&O, respectively.

Table 12 compares the proposed CS algorithm to the other MPPT algorithms. Traditional algorithms such as (In-Cond) may have the advantage of simplicity. However, they are less efficient than the proposed algorithm, which can track the GMPP under partially shaded conditions.

Table 12. Comparison of the proposed technique with other MPPT methods.

Evaluated Parameter	[69-75]	[76]	[77, 78]	[79]	[80]	[6]	InC	Proposed CSA
GMPP tracking capability	Yes	Yes	Yes	Yes	Yes	Yes	No	Yes
Simplicity	Medium	Medium	Medium	Simple	Simple	Simple	Simple	Simple
Efficiency	High	High	High	High	High	High	Low	Very High
Tracking speed	Medium	Medium	Medium	Medium	High	High	High	Very High
Steady-state oscillation	No	No	No	No	No	No	Yes	No
Initial location dependency	Yes	No	Yes	No	No	No	Yes	No
Reliability	Medium	Medium	Medium	Medium	High	High	Low	Very High

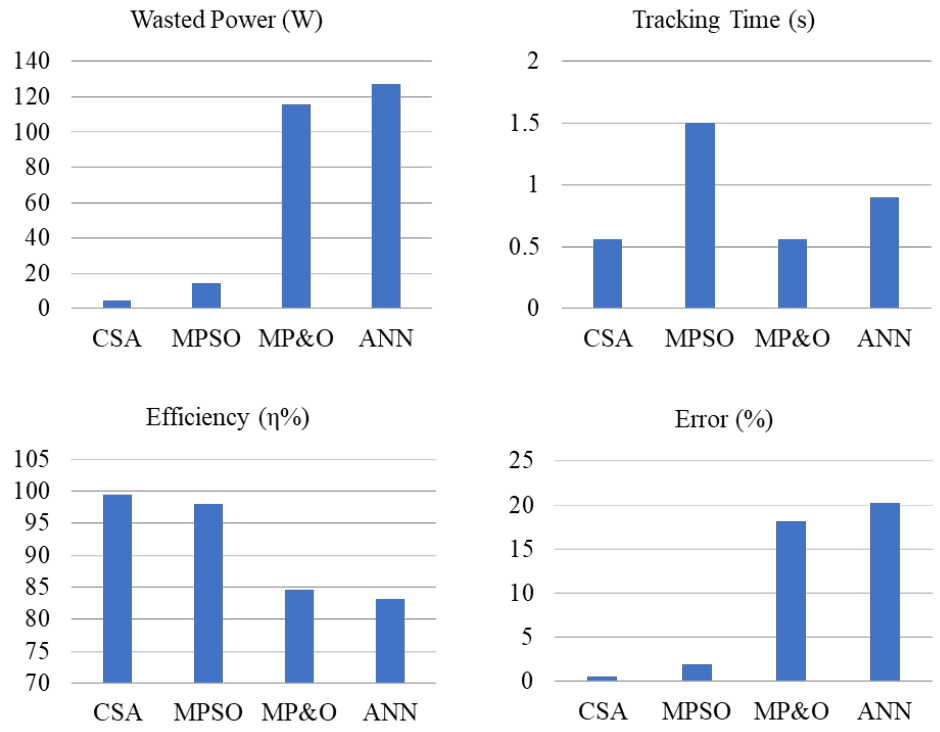

Fig 33. Comparison between statistical results of CSA, MPSO, MP&O, and ANN algorithms.

7 Conclusion

Based on the mathematical model, both photovoltaic cells and the photovoltaic array under partial shading conditions are established and verified using the Matlab/Simulink environmental platform. The model can adjust different parameters such as solar irradiation, cell temperature, and the shading area, which can reflect the photovoltaic modules' output characteristics under different irradiation, temperature, and shading conditions. In the simulation, the results present that the PV array characteristics have only one peak under uniform irradiation conditions, which can be tracked easily. When the PV arrays are exposed to different solar irradiations, the output characteristics will have multiple peaks. The external characteristics equation of PV arrays needs to be described by piecewise function, making the maximum power point tracking more difficult. After that, the boost converter's principle is introduced. Its reliability is proved through the simulation experiments, which lays a basis for the following photovoltaic system simulation model establishment and maximum power point tracking experiment.

In this study, the maximum power point tracking problem is discussed, and based on the comprehensive analysis of artificial intelligence and heuristic algorithms, a control strategy of maximum power point tracking of PV system under partial shading and non-uniform irradiation conditions based on all main algorithms are proposed and discussed in more details. Firstly, by analyzing the PV solar generation system's characteristics, the control objective of maximum PV energy tracking is realized. Then, there is a collection of training data for the ANN controller (voltage, current, duty cycle) to train the MPPT tracker ANN under partial shading and non-uniform irradiation conditions. Finally, the model is trained to present the efficient output parameter for ANN and other methods, which then is used to be associated with MPPT controller which its output is used to control the DC-DC converter to give the reference voltage which can achieve the maximum power point tracking under partial shading and non-uniform irradiation conditions. In this paper, the proposed MPPT method (CSA) system has been modeled and designed to track the maximum power point for the PV system under partial shading conditions. To get the validity of the proposed method performance, the simulation was conducted under different partial shading scenarios. The proposed MPPT control method can track the maximum power successfully for any partial shading condition and scenario. Simulation results demonstrate that the Cuckoo Search Algorithm (CSA) can extract the actual maximum power point rapidly with high efficiency and negligible oscillations around the global point of maximum power under partial shading conditions for various scenarios.

Funding

This study was supported by the Hubei Provincial Natural Science Foundation of China (2015CFA010), the Technology Project of State Grid Company "Soft Connection Mechanism and Modeling of Smart Grid Adapting to the Development of Global Energy Interconnection," and the 111 Projects (B17040).

References

1) Nayak PK, Mahesh S, Snaith HJ, Cahen D. Photovoltaic solar cell technologies: analysing the state of the art. *Nature Reviews Materials*. 2019;4(4):269–285. Available from: https://dx.doi.org/10.1038/s41578-019-0097-0.
2) Kabir S, Bansal R, Nadarajah M. Effects of partial shading on photovoltaic with advanced MPPT scheme. *2012 IEEE International Conference on Power and Energy (PECon)*. 2012;p. 354–359. Available from: 10.1109/PECon.2012.6450237.
3) Xie Y, Weng Q. World energy consumption pattern as revealed by DMSP-OLS nighttime light imagery. *GIScience & Remote Sensing*. 2016;53:265–282. Available from: https://dx.doi.org/10.1080/15481603.2015.1124488.
4) Ram BK, Chidambararaj N. Grasshopper optimization algorithm utilized Xilinx controller for maximum power generation in photovoltaic system. *Evolving Systems*. 2020;p. 1–14. Available from: 10.1007/s12530-020-09333-6.
5) Mora SBS, Paipa EAL, Serrano MAL, Márquez LFB. Performance comparison between PWM and MPPT charge controllers. *Scientia et technica*. 2019;24(1):6–11. Available from: https://dx.doi.org/10.22517/23447214.20681.
6) Ahmed J, Salam Z. A Maximum Power Point Tracking (MPPT) for PV system using Cuckoo Search with partial shading capability. *Applied Energy*. 2014;119:118–130. Available from: https://dx.doi.org/10.1016/j.apenergy.2013.12.062.
7) Ljouad T, Amine A, Rziza M. A hybrid mobile object tracker based on the modified Cuckoo Search algorithm and the Kalman Filter. *Pattern Recognition*. 2014;47(11):3597–3613. Available from: https://dx.doi.org/10.1016/j.patcog.2014.04.003.
8) Shlesinger MF, Klafter J. Lévy walks versus Lévy flights. In: On growth and form. Springer. 1986;p. 279–283. Available from: https://doi.org/10.1007/978-94-009-5165-5_29.
9) Yang XS, Deb S. Engineering optimisation by cuckoo search. *International Journal of Mathematical Modelling and Numerical Optimisation*. 2010;1(4):330–343. Available from: 10.1504/ijmmno.2010.035430.
10) Yang XS, Deb S. Multiobjective cuckoo search for design optimization. *Computers & Operations Research*. 2013;40(6):1616–1624. Available from: 10.1016/j.cor.2011.09.026.
11) Mantegna RN. Fast, accurate algorithm for numerical simulation of Lévy stable stochastic processes. *Physical Review E*. 1994;49(5):4677–4683. Available from: https://dx.doi.org/10.1103/physreve.49.4677.
12) Civicioglu P, Besdok E. A conceptual comparison of the Cuckoo-search, particle swarm optimization, differential evolution and artificial bee colony algorithms. *Artificial intelligence review*. 2013;39(4):315–346. Available from: 10.1007/s10462-011-9276-0.
13) Ibrahim AW, Ding M, Jin X, Dai X, Sarhan MA, Shafik MB, et al. Artificial neural network based maximum power point tracking for PV system. *Chinese Control Conference (CCC)*. 2019;p. 6559–6564. Available from: 10.23919/chicc.2019.8865275.
14) Esram T, Chapman PL. Comparison of Photovoltaic Array Maximum Power Point Tracking Techniques. *IEEE Transactions on Energy Conversion*. 2007;22(2):439–449. Available from: https://dx.doi.org/10.1109/tec.2006.874230.
15) Salam Z, Ahmed J, Merugu BS. The application of soft computing methods for MPPT of PV system: A technological and status review. *Applied Energy*. 2013;107:135–148. Available from: https://dx.doi.org/10.1016/j.apenergy.2013.02.008.
16) Femia N, Petrone G, Spagnuolo G, Vitelli M. Optimization of Perturb and Observe Maximum Power Point Tracking Method. *IEEE Transactions on Power Electronics*. 2005;20:963–973. Available from: https://dx.doi.org/10.1109/tpel.2005.850975.
17) Koutroulis E, Kalaitzakis K, Voulgaris NC. Development of a microcontroller-based, photovoltaic maximum power point tracking control system. *IEEE Transactions on Power Electronics*. 2001;16(1):46–54. Available from: https://dx.doi.org/10.1109/63.903988.
18) Lin CH, Huang CH, Du YC, Chen JL. Maximum photovoltaic power tracking for the PV array using the fractional-order incremental conductance method. *Applied Energy*. 2011;88(12):4840–4847. Available from: 10.1016/j.apenergy.2011.06.024.
19) Masoum MAS, Dehbonei H, Fuchs EF. Theoretical and experimental analyses of photovoltaic systems with voltageand current-based maximum power-point tracking. *IEEE Transactions on Energy Conversion*. 2002;17(4):514–522. Available from: https://dx.doi.org/10.1109/tec.2002.805205.
20) Ahmad J. A fractional open circuit voltage based maximum power point tracker for photovoltaic arrays. *2010 2nd International Conference on Software Technology and Engineering*. 2010;1:1–247. Available from: 10.1109/ICSTE.2010.5608868.
21) Esram T, Kimball JW, Krein PT, Chapman PL, Midya P. Dynamic maximum power point tracking of photovoltaic arrays using ripple correlation control. *IEEE Transactions on Power Electronics*. 2006;21(5):1282–1291. Available from: https://dx.doi.org/10.1109/tpel.2006.880242.
22) Kim IS. Sliding mode controller for the single-phase grid-connected photovoltaic system. *Applied Energy*. 2006;83(10):1101–1115. Available from: 10.1016/j.apenergy.2005.11.004.
23) Papaioannou IT, Purvins A. Mathematical and graphical approach for maximum power point modelling. *Applied Energy*. 2012;91(1):59–66. Available from: https://dx.doi.org/10.1016/j.apenergy.2011.09.005.
24) Al-Amoudi A, Zhang L. Optimal control of a grid-connected PV system for maximum power point tracking and unity power factor. *Institution of Electrical Engineers*. 1998;p. 80–85. Available from: 10.1049/cp:19980504.
25) Piazza MCD, Vitale G. Photovoltaic field emulation including dynamic and partial shadow conditions. *Applied Energy*. 2010;87(3):814–823. Available from: https://dx.doi.org/10.1016/j.apenergy.2009.09.036.
26) Kamran M, Mudassar M, Fazal MR, Asghar MU, Bilal M, Asghar R. Implementation of improved Perturb & Observe MPPT technique with confined search space for standalone photovoltaic system. *Journal of King Saud University-Engineering Sciences*. 2018. Available from: 10.1016/j.jksues.2018.04.006.
27) Radjai T, Gaubert JP, Rahmani L, Mekhilef S. Experimental verification of P&O MPPT algorithm with direct control based on Fuzzy logic control using CUK converter. *International Transactions on Electrical Energy Systems*. 2015;25(12):3492–3508. Available from: https://dx.doi.org/10.1002/etep.2047.
28) Radjai T, Rahmani L, Mekhilef S, Gaubert JP. Implementation of a modified incremental conductance MPPT algorithm with direct control based on a fuzzy duty cycle change estimator using dSPACE. *Solar Energy*. 2014;110:325–337. Available from: https://dx.doi.org/10.1016/j.solener.2014.09.014.
29) Tey KS, Mekhilef S. Modified incremental conductance MPPT algorithm to mitigate inaccurate responses under fast-changing solar irradiation level. *Solar Energy*. 2014;101:333–342. Available from: https://dx.doi.org/10.1016/j.solener.2014.01.003.

30) Tey KS, Mekhilef S. Modified Incremental Conductance Algorithm for Photovoltaic System Under Partial Shading Conditions and Load Variation. *IEEE Transactions on Industrial Electronics*. 2014;61(10):5384–5392. Available from: https://dx.doi.org/10.1109/tie.2014.2304921.
31) Safari A, Mekhilef S. Simulation and Hardware Implementation of Incremental Conductance MPPT With Direct Control Method Using Cuk Converter. *IEEE Transactions on Industrial Electronics*. 2011;58(4):1154–1161. Available from: https://dx.doi.org/10.1109/tie.2010.2048834.
32) Salman S, AI X, WU Z. Design of a P-&-O algorithm based MPPT charge controller for a stand-alone 200W PV system. *Protection and Control of Modern Power Systems*. 2018;3:1–8. Available from: https://dx.doi.org/10.1186/s41601-018-0099-8.
33) Shang L, Guo H, Zhu W. An improved MPPT control strategy based on incremental conductance algorithm. *Protection and Control of Modern Power Systems*. 2020;5:1–8. Available from: https://dx.doi.org/10.1186/s41601-020-00161-z.
34) Chaibi Y, Allouhi A, Salhi M, El-jouni A. Annual performance analysis of different maximum power point tracking techniques used in photovoltaic systems. *Protection and Control of Modern Power Systems*. 2019;4:1–10. Available from: https://dx.doi.org/10.1186/s41601-019-0129-1.
35) El-Khozondar HJ, El-Khozondar RJ, Matter K, Suntio T. A review study of photovoltaic array maximum power tracking algorithms. *Renewables: Wind, Water, and Solar*. 2016;3(1):1–8. Available from: https://dx.doi.org/10.1186/s40807-016-0022-8.
36) Shang L, Zhu W, Li P, Guo H. Maximum power point tracking of PV system under partial shading conditions through flower pollination algorithm. *Protection and Control of Modern Power Systems*. 2018;3:1–7. Available from: 10.1186/s41601-018-0111-3.
37) Soon TK, Mekhilef S. A Fast-Converging MPPT Technique for Photovoltaic System Under Fast-Varying Solar Irradiation and Load Resistance. *IEEE Transactions on Industrial Informatics*. 2015;11(1):176–186. Available from: https://dx.doi.org/10.1109/tii.2014.2378231.
38) Veerachary M, Yadaiah N. ANN based peak power tracking for PV supplied DC motors. *Solar Energy*. 2000;69(4):343–350. Available from: https://dx.doi.org/10.1016/s0038-092x(00)00085-2.
39) Karatepe E, Hiyama T. Artificial neural network-polar coordinated fuzzy controller based maximum power point tracking control under partially shaded conditions. *IET Renewable Power Generation*. 2009;3(2):239–253. Available from: https://dx.doi.org/10.1049/iet-rpg:20080065.
40) Larbes C, Cheikh SMA, Obeidi T, Zerguerras A. Genetic algorithms optimized fuzzy logic control for the maximum power point tracking in photovoltaic system. *Renewable Energy*. 2009;34(10):2093–2100. Available from: https://dx.doi.org/10.1016/j.renene.2009.01.006.
41) Moyo RT, Tabakov PY, Moyo S. Design and Modeling of the ANFIS-Based MPPT Controller for a Solar Photovoltaic System. *Journal of Solar Energy Engineering*. 2021;143(4):143. Available from: https://dx.doi.org/10.1115/1.4048882.
42) Ali MN. A Novel Combination Algorithm of Different Methods of Maximum Power Point Tracking for Grid-Connected Photovoltaic Systems. *Journal of Solar Energy Engineering*. 2021;143(4). Available from: https://doi.org/10.1115/1.4049065.
43) Liu L, Liu C. A novel combined particle swarm optimization and genetic algorithm MPPT control method for multiple photovoltaic arrays at partial shading. *Journal of Energy Resources Technology*. 2013;135(1). Available from: https://doi.org/10.1115/1.4007940.
44) Ahmed NA, Miyatake M. A novel maximum power point tracking for photovoltaic applications under partially shaded insolation conditions. *Electric Power Systems Research*. 2008;78:777–784. Available from: https://dx.doi.org/10.1016/j.epsr.2007.05.026.
45) Sarhan MA, Ding M, Chen X, Ou Y, Wu M. ANFIS Control for Photovoltaic Systems with DC-DC Converters. *Proceedings of the 2017 International Conference on Automation, Control and Robots*. 2017;p. 9–14. Available from: 10.1145/3175516.3175522.
46) Mirjalili S, Mirjalili SM, Hatamlou A. Multi-Verse Optimizer: a nature-inspired algorithm for global optimization. *Neural Computing and Applications*. 2016;27(2):495–513. Available from: https://dx.doi.org/10.1007/s00521-015-1870-7.
47) Chauhan U, Singh V, Kumar B, Rani A. An improved MVO assisted global MPPT algorithm for partially shaded PV system. *Journal of Intelligent & Fuzzy Systems*. 2020;38(5):6715–6726. Available from: https://dx.doi.org/10.3233/jifs-179749.
48) Babu TS, Rajasekar N, Sangeetha K. Modified Particle Swarm Optimization technique based Maximum Power Point Tracking for uniform and under partial shading condition. *Applied Soft Computing*. 2015;34:613–624. Available from: https://dx.doi.org/10.1016/j.asoc.2015.05.029.
49) Ishaque K, Salam Z, Shamsudin A, Amjad M. A direct control based maximum power point tracking method for photovoltaic system under partial shading conditions using particle swarm optimization algorithm. *Applied Energy*. 2012;99:414–422. Available from: https://dx.doi.org/10.1016/j.apenergy.2012.05.026.
50) Mohanty S, Subudhi B, Ray PK. A New MPPT Design Using Grey Wolf Optimization Technique for Photovoltaic System Under Partial Shading Conditions. *IEEE Transactions on Sustainable Energy*. 2016;7(1):181–188. Available from: https://dx.doi.org/10.1109/tste.2015.2482120.
51) Agwa AM, Mahmoud IY. Photovoltaic Maximum Power Point Tracking by Artificial Neural Networks. *Journal of Multidisciplinary Engineering Science and Technology*. 2017;4(1). Available from: https://doi.org/10.1155/2012/506709.
52) Matagne E, Chenni R, Bachtiri R. A photovoltaic cell model based on nominal data only. *2007 International conference on power engineering, energy and electrical drives*. 2007;p. 562–565. Available from: 10.1109/powereng.2007.4380173.
53) Rashid MH. Simulation of Power Electronic Circuits. In: Modern Electrical Drives. Springer. 2000;p. 453–489. Available from: https://doi.org/10.1007/978-94-015-9387-8_21.
54) Al-Wesabi I, Shafik MB, Ding M, Sarhan MA, Fang Z, Alareqi AG, et al. PV maximum power-point tracking using modified particle swarm optimization under partial shading conditions. *Chinese Journal of Electrical Engineering*. 2020;6(4):106–121. Available from: https://dx.doi.org/10.23919/cjee.2020.000035.
55) de Cardona MS, López LM. Performance analysis of a grid-connected photovoltaic system. *Energy*. 1999;24(2):93–102. Available from: https://dx.doi.org/10.1016/s0360-5442(98)00084-x.
56) Esram T, Chapman PL. Comparison of Photovoltaic Array Maximum Power Point Tracking Techniques. *IEEE Transactions on Energy Conversion*. 2007;22(2):439–449. Available from: https://dx.doi.org/10.1109/tec.2006.874230.
57) Cheikh MA, Larbes C, Kebir GT, Zerguerras A. Maximum power point tracking using a fuzzy logic control scheme. *Revue des energies Renouvelables*. 2007;10(3):387–395. Available from: https://www.cder.dz/download/Art10-3_8.
58) Dutta A, Barua N, Saha A. Design of an arduino based Maximum Power Point Tracking (MPPT) solar charge controller. 2016. Available from: http://hdl.handle.net/10361/6396.
59) Pathak PK, Yadav AK, Alvi PA. Advanced Solar MPPT Techniques Under Uniform and Non-Uniform Irradiance: A Comprehensive Review. *Journal of Solar Energy Engineering*. 2020;142(4). Available from: https://dx.doi.org/10.1115/1.4046090.
60) Enslin JHR, Wolf MS, Snyman DB, Swiegers W. Integrated photovoltaic maximum power point tracking converter. *IEEE Transactions on Industrial Electronics*. 1997;44(6):769–773. Available from: https://dx.doi.org/10.1109/41.649937.
61) Huynh DC, Dunnigan MW. Development and Comparison of an Improved Incremental Conductance Algorithm for Tracking the MPP of a Solar PV Panel. *IEEE Transactions on Sustainable Energy*. 2016;7(4):1421–1429. Available from: https://dx.doi.org/10.1109/tste.2016.2556678.

62) Kamran M, Mudassar M, Fazal MR, Asghar MU, Bilal M, Asghar R. Implementation of improved Perturb & Observe MPPT technique with confined search space for standalone photovoltaic system. *Journal of King Saud University-Engineering Sciences*. 2018. Available from: 10.1016/j.jksues.2018.04.006.
63) Liu L, Liu C. A novel combined particle swarm optimization and genetic algorithm MPPT control method for multiple photovoltaic arrays at partial shading. *Journal of Energy Resources Technology*. 2013;135(1). Available from: 10.1115/1.4007940.
64) Liu L, Liu C, Gao H. A novel improved particle swarm optimization maximum power point tracking control method for photovoltaic array by using current calculated predicted arithmetic under partially shaded conditions. *Journal of Renewable and Sustainable Energy*. 2013;5(6). Available from: 10.1063/1.4858615.
65) Li H, Liu LQ. A novel particle swarm optimization maximum power point tracking control method based on the direct current voltage superposition principle under partially shaded conditions. *Journal of Vibration and Control*. 2014;20(9):1356–1360. Available from: 10.1177/1077546312471068.
66) Rajabioun R. Cuckoo Optimization Algorithm. *Applied Soft Computing*. 2011;11(8):5508–5518. Available from: https://dx.doi.org/10.1016/j.asoc.2011.05.008.
67) Soneji H, Sanghvi RC. Towards the improvement of cuckoo search algorithm. *2012 World Congress on Information and Communication Technologies*. 2012;p. 878–883. Available from: 10.1109/WICT.2012.6409199.
68) Yang XS, Deb S. Cuckoo search via Lévy flights. *2009 World congress on nature & biologically inspired computing (NaBIC)*. 2009;p. 210–214.